# 3 ANALYSIS OF ALL AVAILABLE ZODIACAL LIGHT OBSERVATIONS 4 4 FINAL REPORT 6

Prepared for

NATIONAL AERONAUTICS AND SPACE ADMINISTRATION
NASA Contract NASw 1206

25

Prepared by


6 R.S. Powell, P.D. Woodson III, M.A. Alexander
R.R. Circle, A.G. Konheim, D.C. Vogel, and T.W. McElfresh 9
1 ET AL

2 SPACE SYSTEMS LABORATORY 3
1 MELPAR, INC.
7700 Arlington Boulevard
Falls Church, Virginia 22046


9 February 1967 10


N67-19931
(ACCESSION NUMBER)
66
(PAGES)
CR-82936
(NASA CR OR TMX OR AD NUMBER)
(THRU)
1
(CODE)
30
(CATEGORY)
FACILITY FORM 602

TABLE OF CONTENTS


| | | Page |
|---|---|---|
| ABSTRACT | | 5 |
| 1. | INTRODUCTION | 6 |
| 2. | A BELT MODEL OF THE INTERPLANETARY DUST ENSEMBLE | 9 |
| 3. | DEDUCTIONS FROM THE OBSERVATIONS USING THE BELT MODEL | 15 |
| 4. | THE COLOR OF THE ZODIACAL LIGHT AS ESTIMATED FROM THE BELT MODEL | 29 |
| 5. | NONSPHERICAL PARTICLES | 32 |
| 6. | CONCLUSIONS | 40 |
| REFERENCES | | 43 |

LIST OF ILLUSTRATIONS


| Figure | | Page |
|---|---|---|
| 1 | Belt Distribution Map. The size distribution of particles in each belt as derived from the various zodiacal light observations are shown in figures 8-11. | 10 |
| 2a | Comparative Theoretical (Top) and Observational (Bottom) $\Delta(\varepsilon) = B_1 - B_2$ | 13 |
| 2b | Comparative Theoretical (Right) and Observational (Left) Brightness, $B_3$ | 14 |
| 3 | Comparison Between Observations of Weinberg and Theoretical Model | 16 |
| 4 | Comparison Between the Observations of Blackwell-Ingham and Theoretical Model | 17 |
| 5 | Comparison Between Observations of Divari-Asaad | 18 |
| 6 | Comparison Between the Observations of Robley and Theoretical Model | 19 |
| 7 | Comparison Between Observations of Behr-Siedentopf and Theoretical Model | 20 |
| 8 | Theoretical Model, Mercury-Venus Belt | 21 |
| 9 | Theoretical Model, Venus-Earth Belt | 22 |
| 10 | Theoretical Model, Earth Ring | 23 |
| 11 | Theoretical Model, Earth-Mars Belt. | 24 |
| 12 | Average Size Distribution Derived from the Belt Model (Powell & Woodson) Compared to Previous Estimates | 27 |
| 13 | Superposition of all Derived Size Distributions | 28 |
| 14 | Color of the Zodiacal Light as Predicted from the Belt Model (as derived from Weinberg's single-color observations) | 30 |
| 15 | Optical Character of MgO Cubes | 35 |
| 16 | Optical Character of ZnO Fourlings. The equivalent sphere size distribution was constructed to match the angular scattering measured from fourlings at $\lambda = 546$ mu. Notice that the scattering from fourlings at $\lambda = 365$ mu is not the same as predicted from the equivalent spheres | 36 |

LIST OF ILLUSTRATIONS (Continued)


| Figure | | Page |
|---|---|---|
| 17 | Optical Character of Imperfect ZnO Fourlings. Although the angular character and wavelength dependence of the light scattered by imperfect fourlings is the same as equivalent spheres (except at $30^{\circ} < \theta < 80^{\circ}$ where the wavelength dependence deviates), the equivalent spheres are larger. | 37 |

ABSTRACT

A model of the interplanetary dust ensemble is derived which explains many of the inconsistencies in the zodiacal light observations. It is shown that the number density of particles is nearly independent of distance from the sun in the region between Mercury and Mars but is possibly zero beyond Mars. Further, it is shown that the size distribution of the interplanetary dust changes slightly with time and distance from the sun. Finally, it is shown that the ensemble consists of particles with radii less than 1.1 micron. A few larger particles certainly exist but they do not affect the zodiacal light. The electron density in the region beyond Mercury is arbitrary.

## 1. INTRODUCTION

All previous analysts of the zodiacal light observations have made two drastic assumptions concerning the nature of the interplanetary dust ensemble. The first assumption is that the size distribution of the interplanetary dust is the same at all points throughout the solar system. The second is that the number density of the particles at a given distance, r, from the sun can be represented by a monotonic function of r. These assumptions have been necessary in order to simplify the scattering equations which relate the measured brightness and polarization of the zodiacal light to the theoretical functions which describe the optical properties of small particles (Mie, 1908 and Born/Wolf, 1964).

Both assumptions are embodied in the mathematical expression for the number density of the interplanetary dust used in the detailed analysis of Blackwell/Ingham's and Weinberg's observations by Giese/Siedentopf (1962), Giese (1963), and Little et al. (1965). The expression is:*

$$N(r,a) = N(a_o)(a/a_o)^{-p}(R/r)^{v} \qquad (1)$$

It was initially used by Allen (1947) and Van de Hulst (1947) to demonstrate the necessity of considering the diffraction component of the light scattered by the dust. It has no fundamental significance.

The model of the interplanetary dust ensemble corresponding to equation (1) can be rationalized to fit the models derived from dynamic considerations (see, for example, Southworth, 1964; Harwit, 1963; Wyatt/Whipple, 1950), but any number of more complicated models are possible.

*N(r,a) is the number density of particles with radius, a, at distance r from the sun. $a_o$, p and v are constants deduced from the observations.

For example, the Mariner IV data indicate that the number density may be an oscillating function of r (Alexander et al., 1965). Even more complicated models seem reasonable on the basis of observations supporting the hypothesis of an earth centered belt (Divari, 1964). Equation (1) does not account for observed meteor showers nor does it seem reasonable in view of the fact that forces due to radiation pressure and the Poynting-Robertson effect are very sensitive to particle size (Wyatt/Whipple, 1950; Beard, 1959).

There is a third assumption usually made that the interplanetary dust ensemble does not contain a significant number of submicron size particles. Particles with radii less than 0.1 to 0.8 microns (depending on the absorption coefficient and mass density) are supposedly blown out of the solar system by the sun's photon and corpuscular radiation. However, as pointed out by Shapiro et al. (1966), Belton (1966), and others, the calculation of the resultant forces on an interplanetary particle is not so simple as some of us pretend. They mention several mechanisms which modify the effects of radiation pressure. Also, there are several possible sources which give a continual supply of submicron particles. For example, the fluffy particles of Soberman and Hemenway (1961) can be pulled toward the sun by the Poynting-Robertson effect and broken up (Giese, 1963) possibly by charge effects induced as they approach the region of the electron corona, or converted to small particles by surface evaporation (Belton, 1966). Fesenkov (1963) alludes to the idea that there exist many asteroid-like bodies orbiting throughout the solar system. These could continually produce particles with radii smaller than those set by radiation pressure. Although the possibility that comets are a source of submicron particles has been questioned

(Southworth, 1964), such particles fit the available observations of comet Arend-Roland and Mrkos (Donn et al., 1967).

Another objection to submicron interplanetary dust is based on the argument that such particles are incompatible with the observed color of the F corona (Elsasser, 1965; Southworth, 1964). However, there is no reason to assume that the size distribution of dust close to the sun is the same as that in the zodiacal light.*

Many investigators assume that the zodiacal light would be much bluer than sunlight if the interplanetary ensemble contained large numbers of submicron particles. Tanabe (1967) and Karyagina (1961) have shown that the zodiacal light is bluer than sunlight at elongations $15^{\circ}$-$40^{\circ}$ and $40^{\circ}$-$50^{\circ}$, respectively. As we will show later, a submicron particle model of the interplanetary dust ensemble is compatible with their spectral measurements.

Having cast dispersions on all the usual assumptions used for analysis of the zodiacal light observations, thereby adding more confusion to an already confusing problem, we now proceed to present a model of the interplanetary dust which is just as arbitrary. We do this for two reasons: first, we want to test the uniqueness of previous analytic fits to the zodiacal light observations and second, we want to demonstrate that the apparent disagreement among various observers (as reviewed by Weinberg, 1964, and Gillett, 1966) may not be as serious as we all thought. We shall present a model of the interplanetary dust which fits most of the available observations.

*In fact, large particles are continually being "pulled" into smaller and smaller volume around the sun by the Poynting-Robertson forces. Submicron particles are not.

## 2. A BELT MODEL OF THE INTERPLANETARY DUST ENSEMBLE

Let us arbitrarily separate the interplanetary space (in the ecliptic) into a system of belts, the boundry of each belt coinciding with the orbits of the planets as shown in figure 1. Let us assume that the $k^{th}$ belt is populated with particles having any size distribution at all, i.e., we assume that all particle sizes and refractive indices (real and complex) are possible and that the size distribution, number density, and chemical composition of particles in one belt are completely independent of the same quantities in another. We will assume for now that the particles are spherical.

Using such a model, it is possible to deduce the size distribution of particles in each belt from the many single color observations of the zodiacal light. The inversion is based on the mathematical method of Powell and Donn (1967). Although the necessary inversions of the familiar integral equations (Giese, 1963; Van de Hulst, 1947) are accomplished through approximations, the results are as accurate as the Mie theory allows. We point out that the method has been applied to observations of comet Arend-Roland and Mrkos by Donn and Powell (to be published) and the results checked according to the exact Mie theory by Remy-Battiau (to be published). We found that the particles in both comets were dielectric -- definitely not iron as Liller (1960) suggested. The method has been checked further by reproducing the analytic results of Giese and Siedentopf (1962).

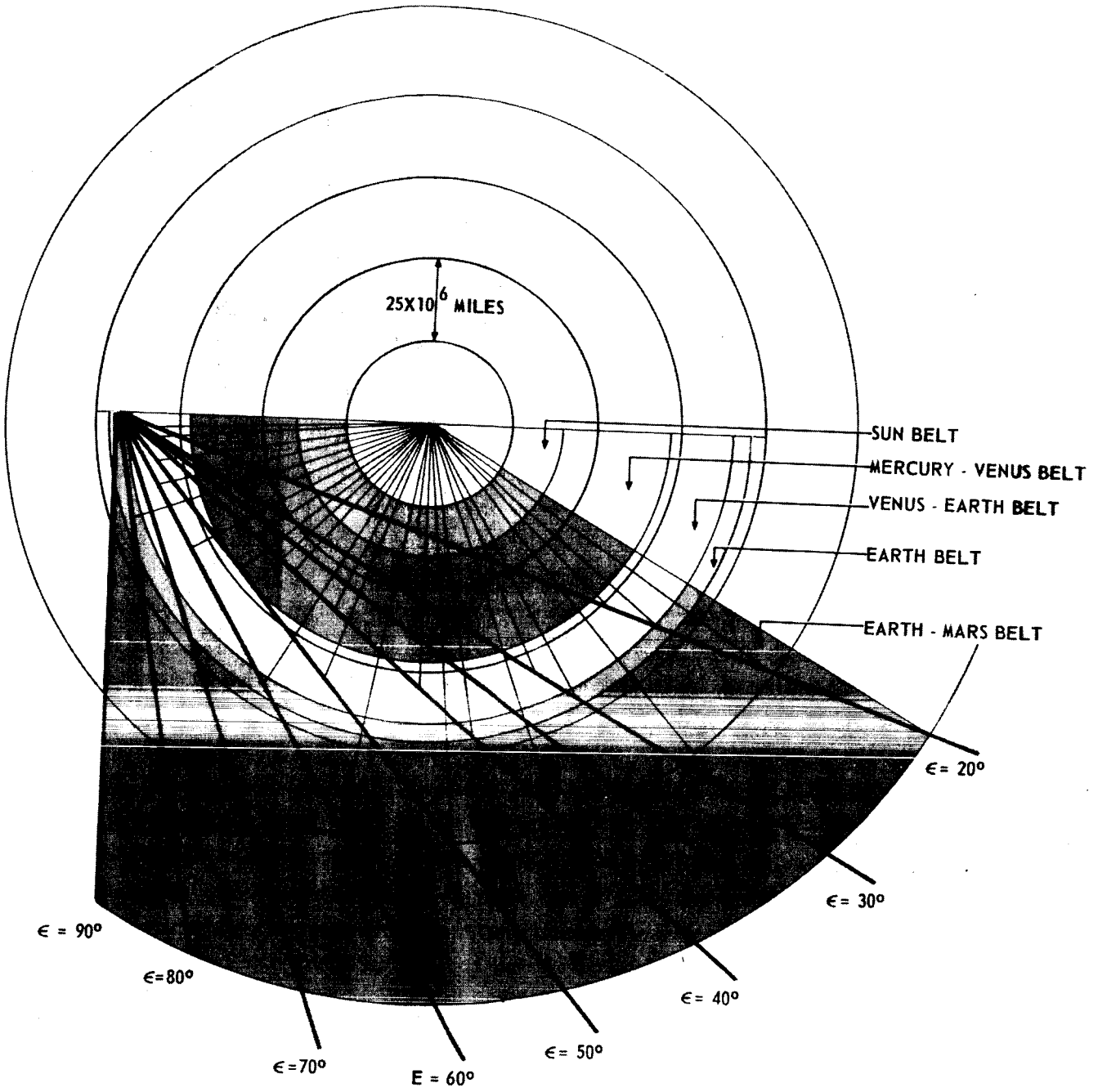


Figure 1. Belt Distribution Map. The size distribution of particles in each belt as derived from the various zodiacal light observations are shown in figures 8-11.

Our method does not allow a direct fit of the polarization function

$$P = \frac{B_1 - B_2}{B_1 + B_2} \tag{2}$$

as used in the review of observations by Weinberg (1964). Instead, we use the Delta parameter:

$$\Delta = B_1 - B_2 = PB_3 \tag{3}$$

which is the difference between the brightnesses measured with electric vectors perpendicular and parallel to the scattering plane, respectively. The delta parameter is also the product of the measured polarization P, and the measured brightness, $B_3 = B_1 + B_2$.

The delta parameter corresponds more closely to the quantities actually measured than does the polarization in the sense that the delta parameter is a combination of two separately measured variables, whereas the polarization is a combination of three. In this regard we point out that the experimental corrections for the measured brightness, $B_3$, are radically different than those for the measured delta, $B_1 - B_2$, and that the brightness is an absolute measurement, whereas delta is relative. These factors may lead to large discrepancies in various observations of the polarization but small discrepancies in various observations of the delta parameter. For example, over-correction of the measured brightness, $B_3$, leads to a value for the polarization, $(B_1 - B_2)/B_3$, which is too low and vice versa. This correlation might be expected to show up in the observations. It does in a general way. The polarization measured by

Blackwell/Ingham and Elsasser is much higher than Weinberg's but Weinberg's brightness is higher (Weinberg, 1964). When one corrects the polarization measured by Blackwell/Ingham and Elsasser by the ratio of their brightness to Weinberg's, the large discrepancies disappear. Of course, the correction is not as simple as the above discussion indicates. On the other hand, we emphasize that theoretical fits to the delta parameter are probably more realistic than fits to the polarization. A comparison of observations, $\Delta(\epsilon)$, according to various representative observers is shown in the bottom of figure 2A. The corresponding Brightness observations are shown in the left-hand graph of figure 2B.

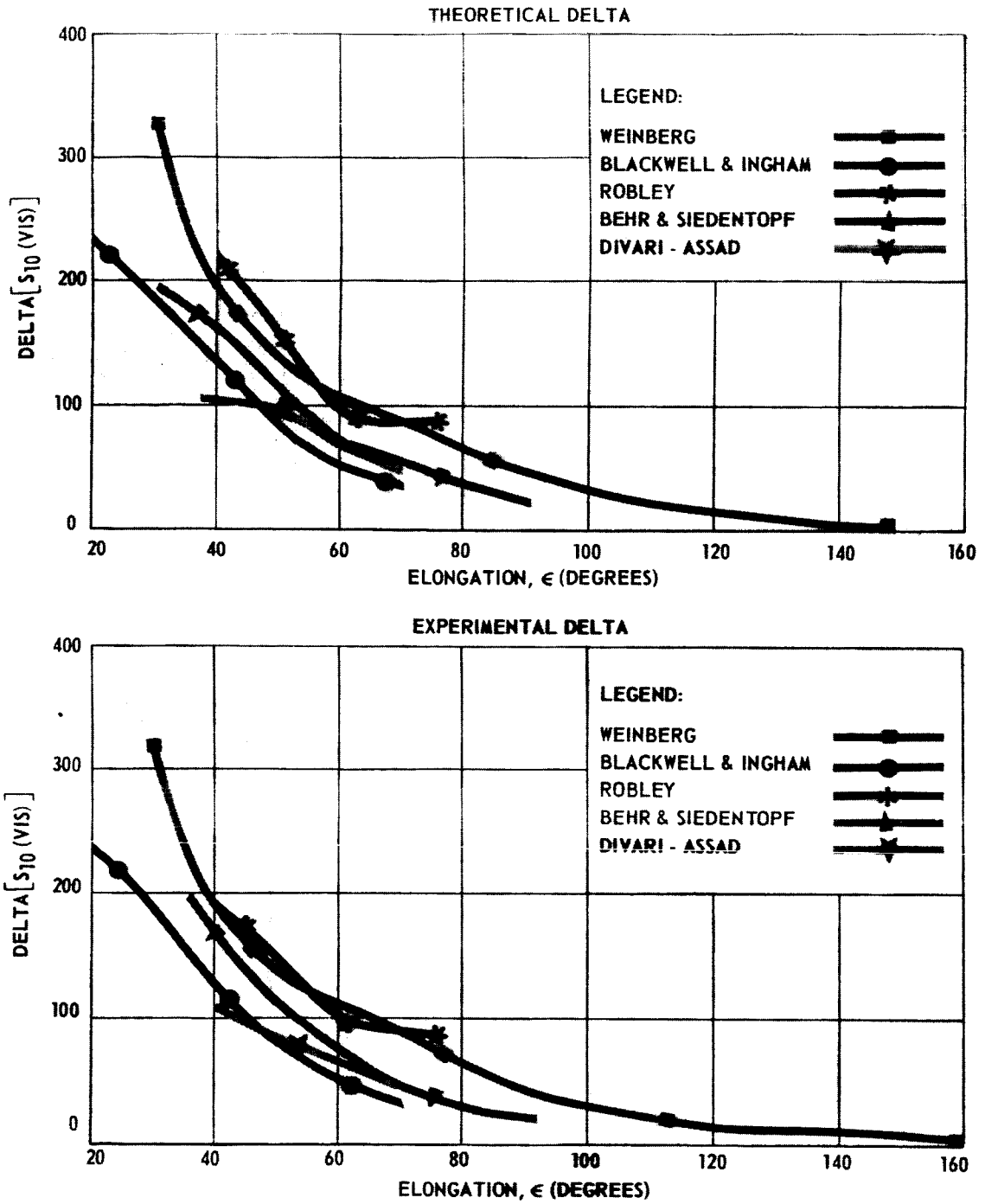


Figure 2a. Comparative Theoretical (Top) and Observational (Bottom) $\Delta(\epsilon) = B_1 - B_z$

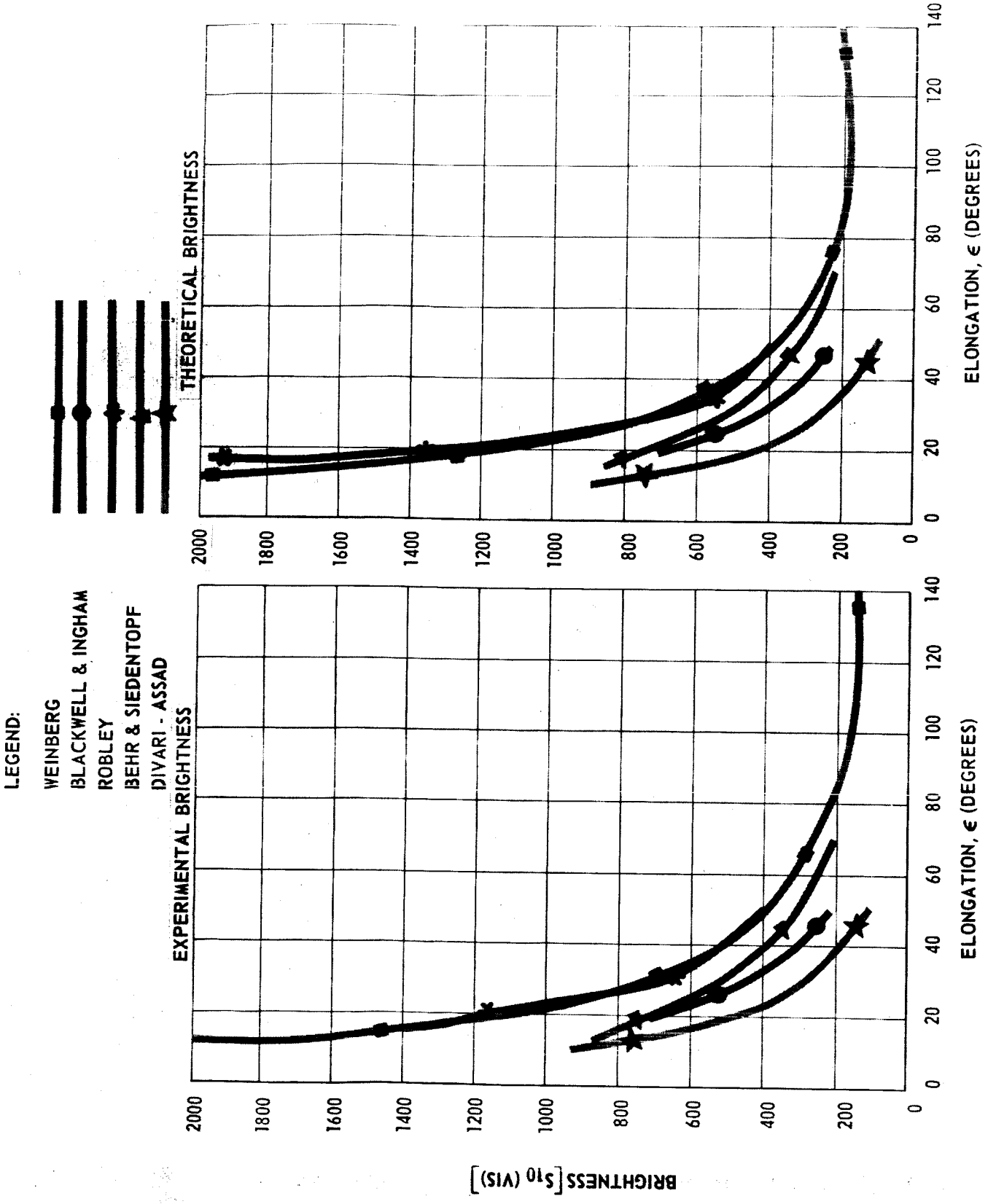


Figure 2b. Comparative Theoretical (Right) and Observational (Left) Brightness, $B_3$.

## 3. DEDUCTIONS FROM THE OBSERVATIONS USING THE BELT MODEL

The observations of Weinberg (1964), Blackwell/Ingham (1961), Divari/Asaad (1960), Robley (1962), and Behr/Siedentopf (1953) are shown in figures 3 through 7, respectively. The theoretical curves from the belt model are shown superimposed on the observational curves. We have been able to match Weinberg's and Blackwell/Ingham's curves exactly. The observations of Robley and Divari/Asaad can be matched approximately within the experimental error. Behr and Siedentopf's observations cannot be matched precisely unless one assumes that Venus sweeps out particles near its orbit.

The observations shown in figures 3 through 7 and the conclusions drawn therefrom are representative of all other available observations (Elsasser, 1958; Huruhata, 1951; Barbier, 1955; Smith, et al., 1965; Beggs et al., 1964; Walstencraft/Rose, 1967; and Gillett/Ney, 1966). We have not analyzed the data of Peterson (1961) and Dufay (1925). Peterson's data do not extend close enough to the sun for our purposes and Dufay's measurements were made before there was sufficient knowledge concerning atmospheric corrections.

The size distribution and refractive indices of the particles in each belt as derived independently from each of the observations are shown in figure 8 (Mercury-Venus), figure 9 (Venus-Earth), figure 10 (Earth), and figure 11 (Earth-Mars).

The characteristics of the interplanetary dust as deduced from all zodiacal light observations are remarkably similar. All observations indicate that the radii of the particles lie in the range 0.08 to 1.5 microns and that the decrease in number density with increasing particle size is

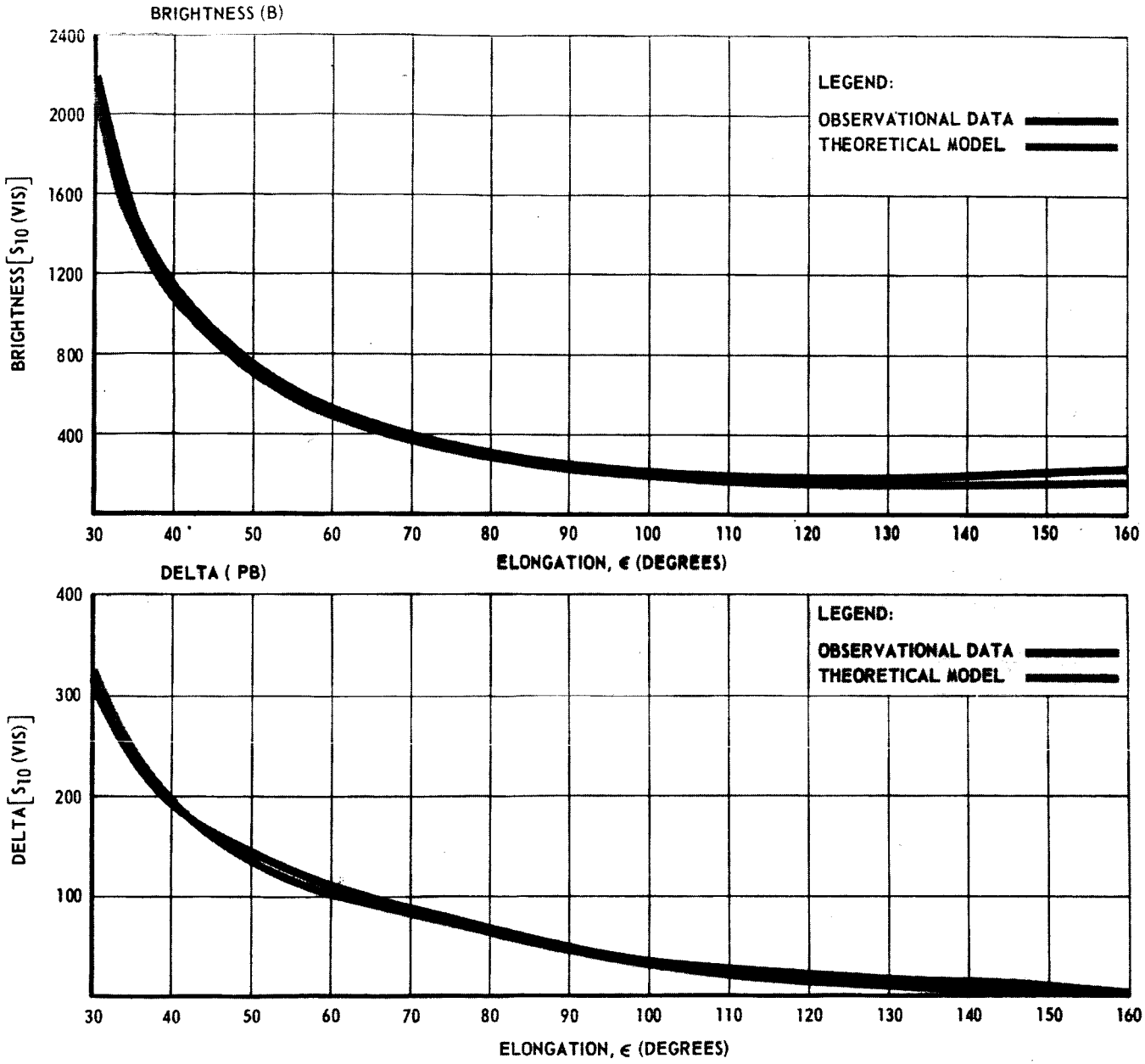


Figure 3. Comparison Between Observations of Weinberg and Theoretical Model.

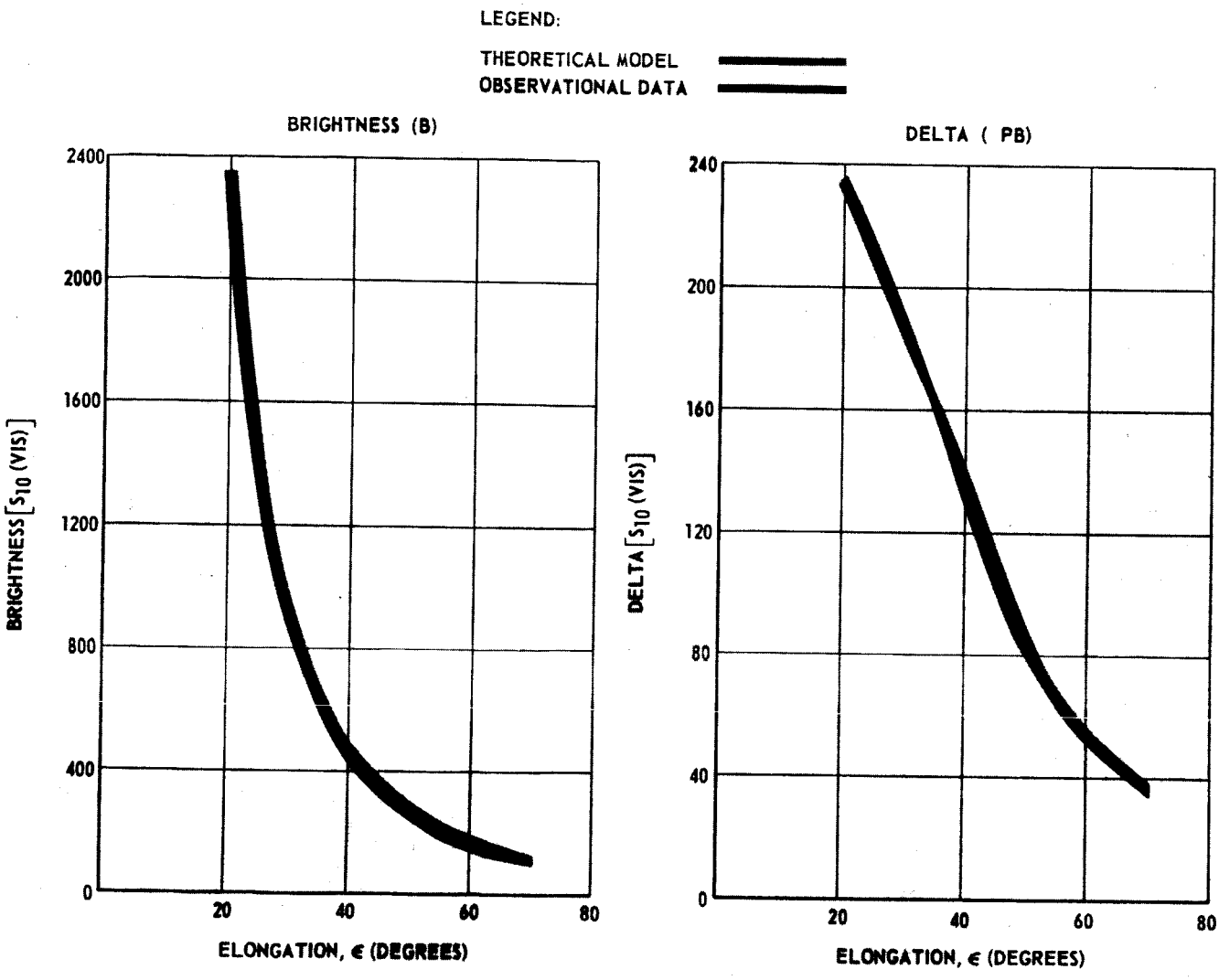


Figure 4. Comparison Between the Observations of Blackwell-Ingham and Theoretical Model.

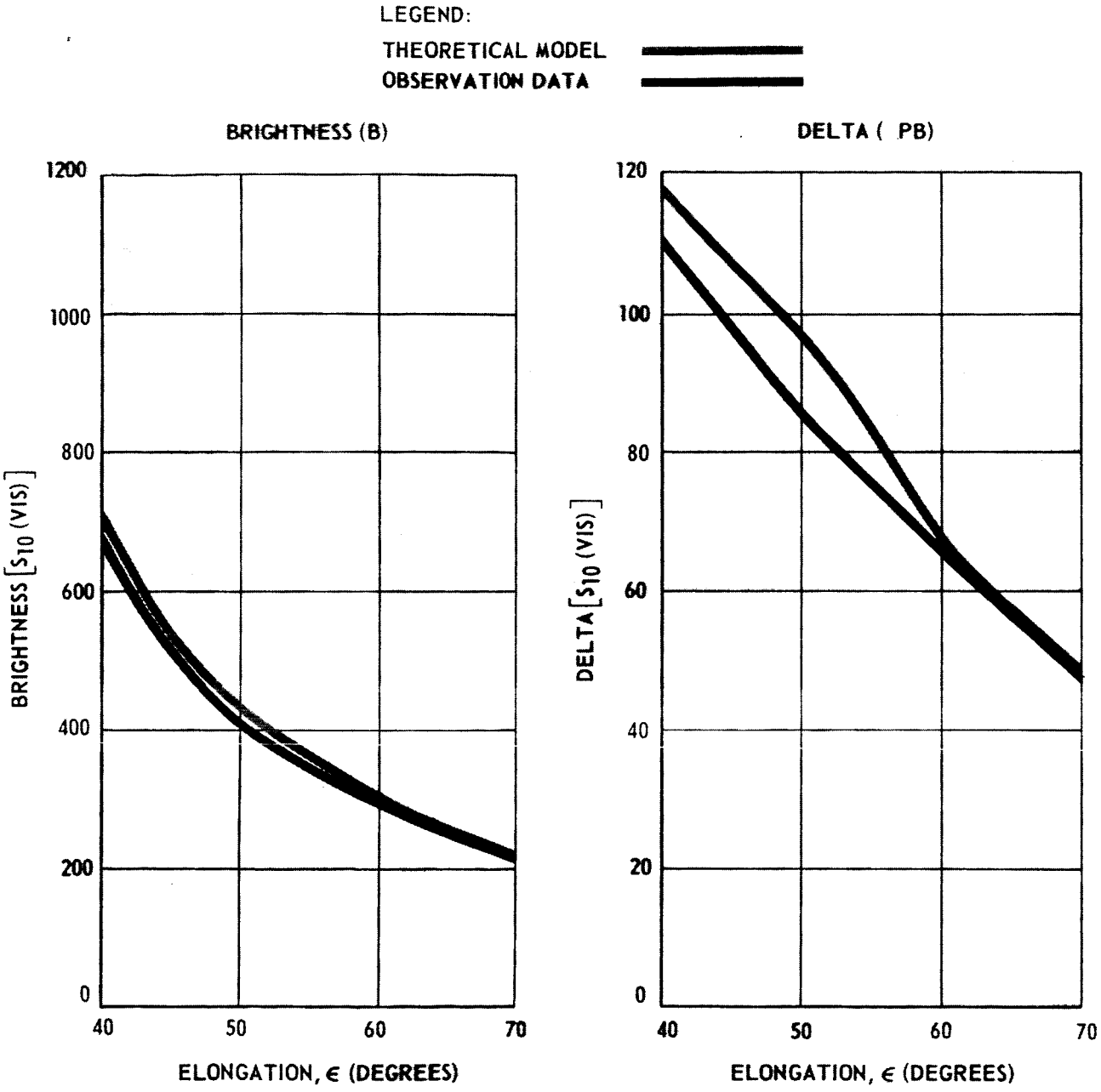


Figure 5. Comparison Between Observations of Divari-Assad

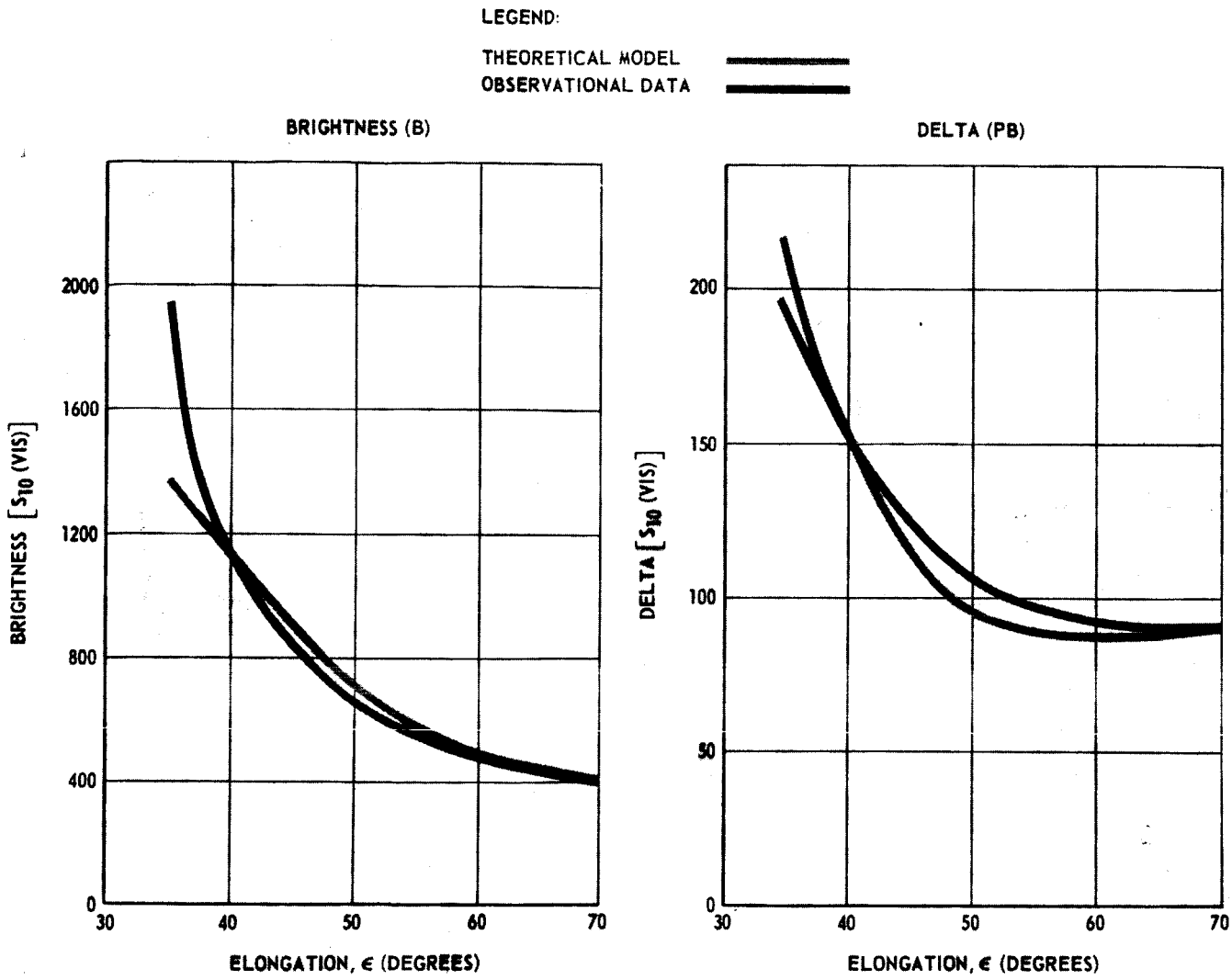


Figure 6. Comparison Between the Observations of Robley and Theoretical Model.

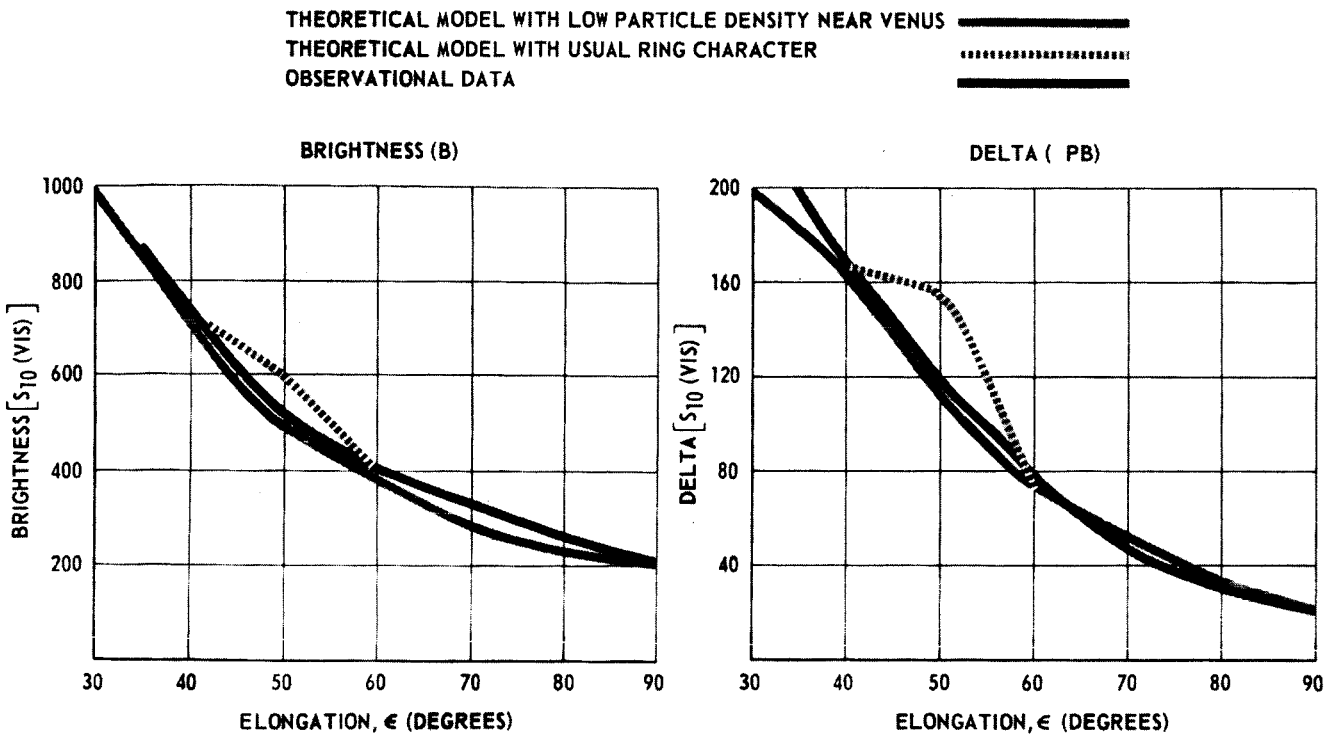


Figure 7. Comparison Between Observations of Behr-Siedentopf and Theoretical Model.

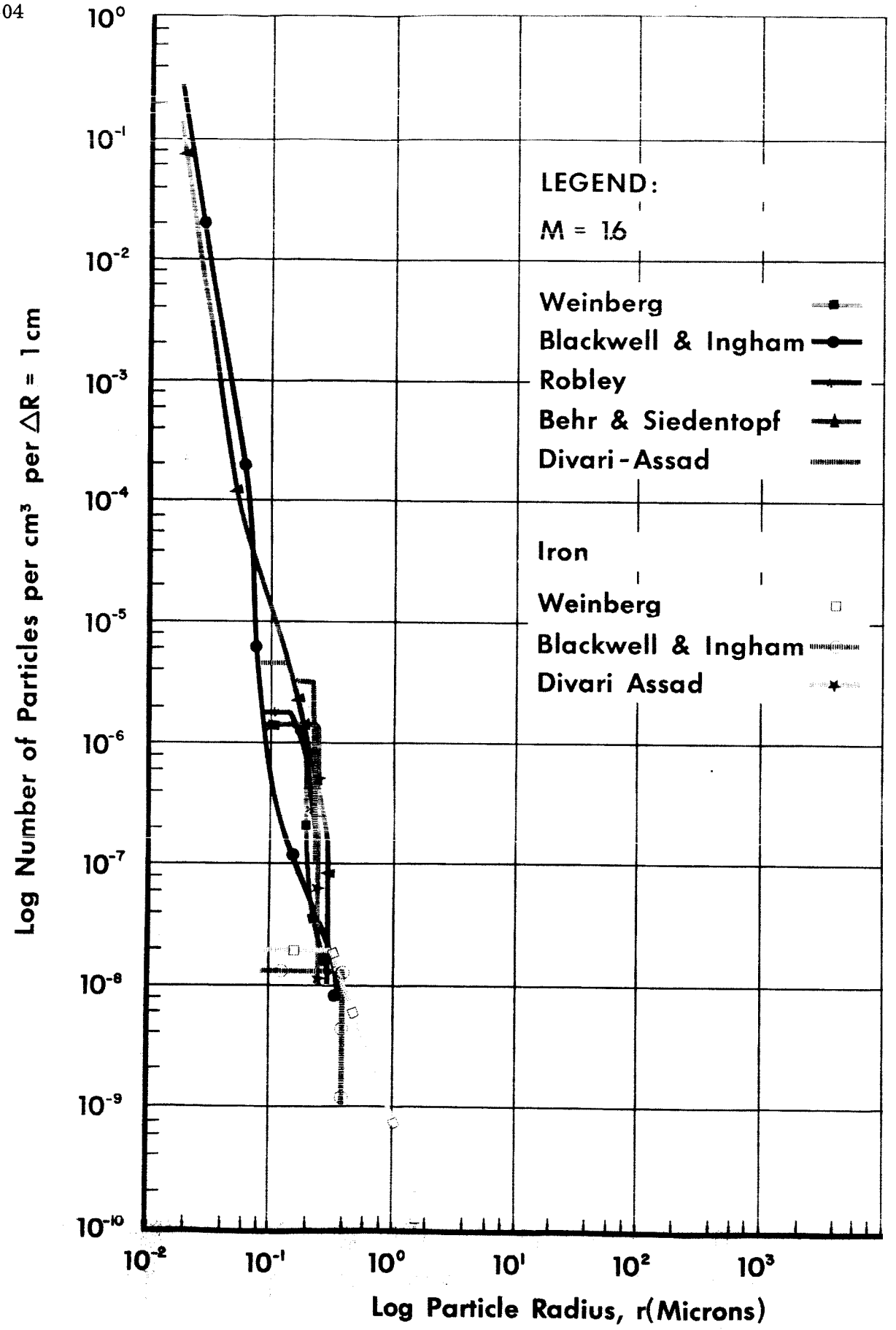


Figure 8. Theoretical Model, Mercury-Venus Belt.

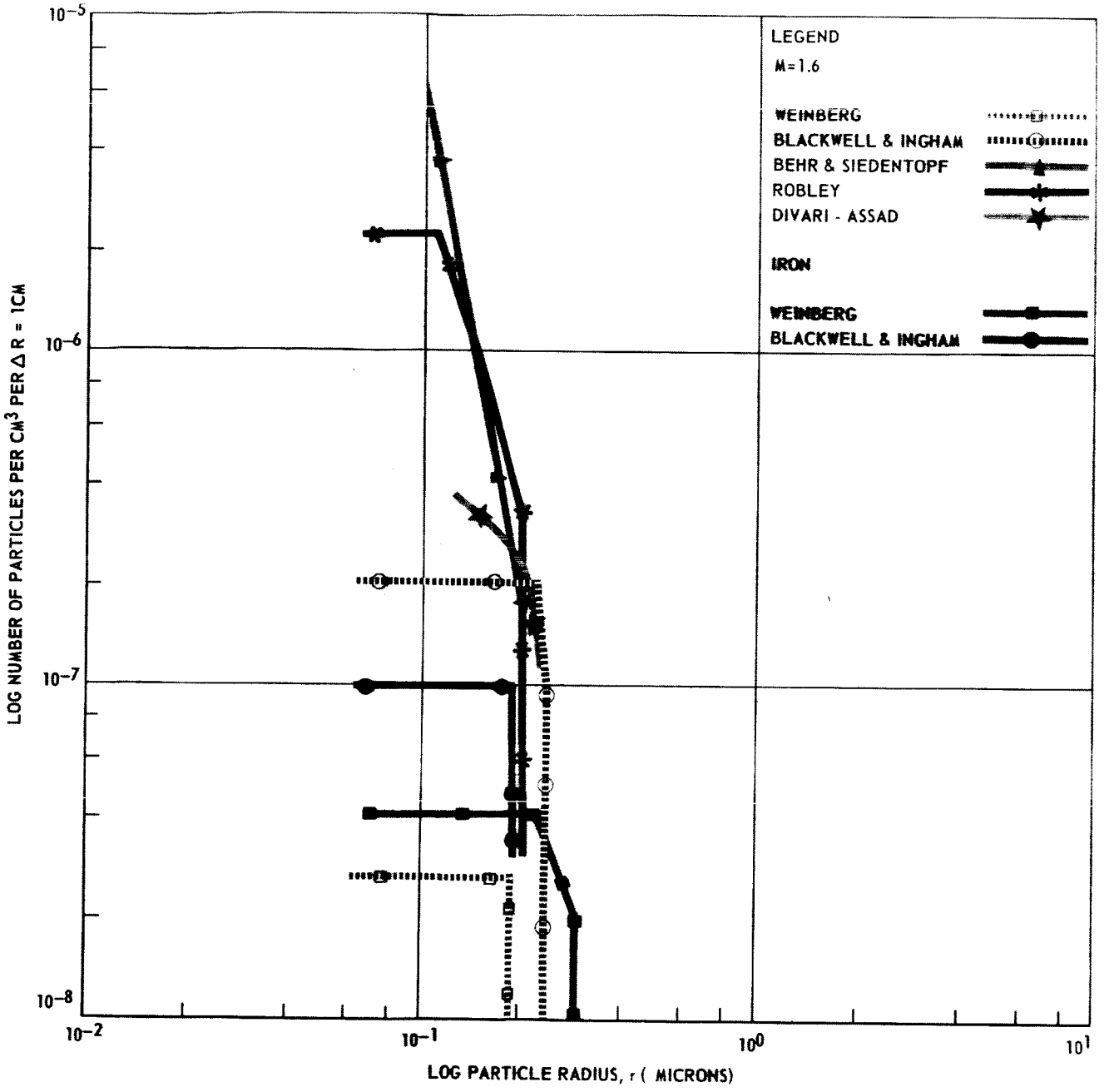


Figure 9. Theoretical Model, Venus-Earth Belt.

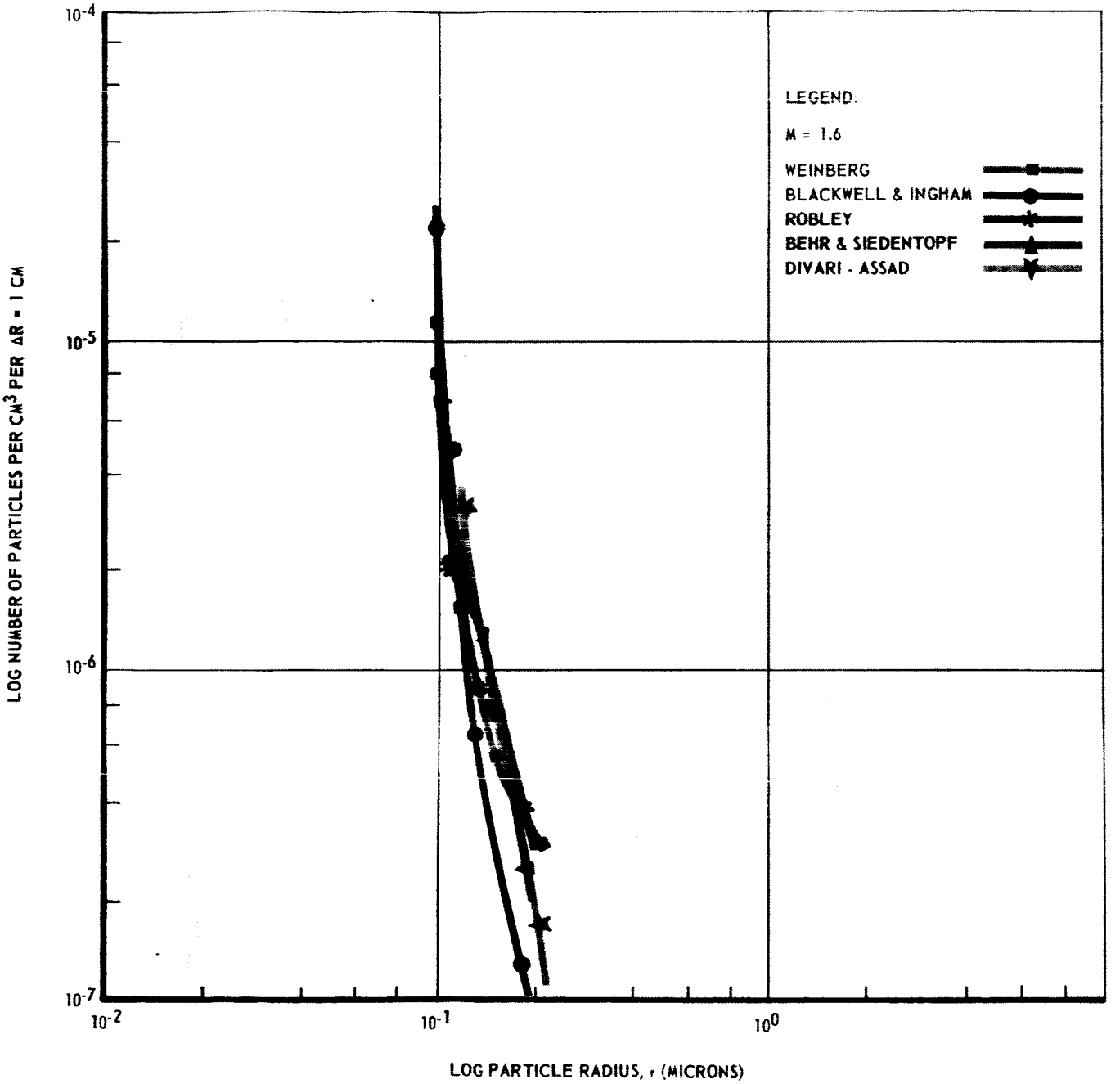


Figure 10. Theoretical Model, Earth Ring.

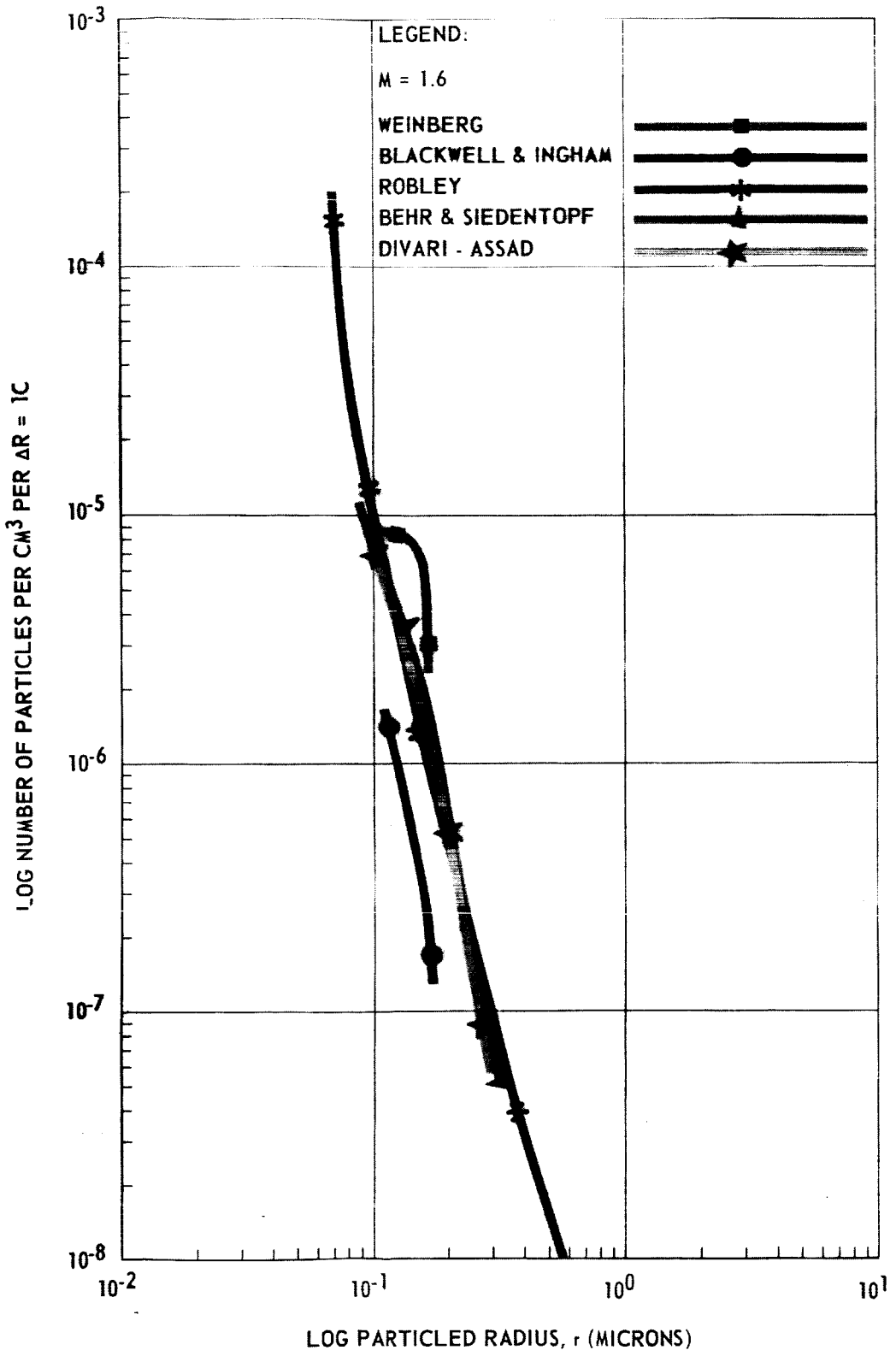


Figure 11. Theoretical Model, Earth-Mars Belt.

very steep. The large differences in the observations can be explained by slight differences in the size and composition of the interplanetary particles.*

In the region between Mercury and Venus (figure 8), the observations of Weinberg, Blackwell/Ingham, and Divari/Asaad all require the existence of iron particles in addition to dielectrics. Most of these iron particles have radii less than 1 micron but more than 0.08μ. Notice that the number density of iron particles is lower than that for dielectrics and that the iron particles size is larger. Notice also that the observations of Blackwell/Ingham and Behr/Siedentopf require the existence of a large number of very small particles with radii less than 0.1μ - at least a factor of 100 more than required by the other observers. The refractive index of dielectric particles is between $m = 1.4$ and $m = 1.8$ for all observers.

In the region between Venus and Earth the dielectric particles ($1.4 \leq m \leq 1.8$) have radii $0.08 \leq a \leq 0.3$ microns. Behr/Siedentopf, Divari/Asaad, and Robley require a higher proportion of small particles than either Weinberg or Blackwell/Ingham. Weinberg and Blackwell/Ingham require iron particles. Again, these are larger and less numerous than the dielectrics.

All observations also lead to similar conclusions concerning the nature of the dust near Earth's orbit. The particles are all dielectrics ($1.4 \leq m \leq 1.8$) and very small (0.08 to 0.2 microns radii). Weinberg's observations require that particles near the Earth's orbit ($0.9 \leq r \leq 1.1$ A.U.)

*Of course there is no way to determine whether or not electrons are present from analysis of single-color observations. Particles with radii less than 0.08 micron scatter like electrons. Thus, the number density of such particles as plotted in figures 8 through 11 may be multiplied by $10^7$ to $10^{10}$ (depending on size) to estimate the equivalent number of electrons.

have slightly different size distribution than those in the Venus-Earth belt. The slope (number density vs particle size) is steeper than previously estimated. For comparison we present our results with previous estimates in figure 12.

In the region between Earth and Mars (figure 11) we find again that all particles are dielectric with radii in the range 0.08 to 0.6. The size distribution which fits Robley's observations has the highest proportion of small particles. The size distributions corresponding to the observations of Weinberg and Blackwell/Ingham require the same narrow range of particle radii, $0.1 \leq a \leq 0.2$, but Weinberg's number density is greater by a factor between 7 and 20.

No particles are required in the space beyond Mars to explain the existing observations. On the other hand, the size and radial distribution of particles beyond Mars may be similar to those interior to Mars, but the number density must be less by at least a factor of ten.

As can be seen by comparing figures 8 through 11, the size distribution is roughly the same throughout the region from Mercury to Mars. Furthermore, the number density is nearly independent of distance from the sun. The accuracy of these two statements can be judged from figure 13 where the size distributions derived from all observations in all belts are superimposed.

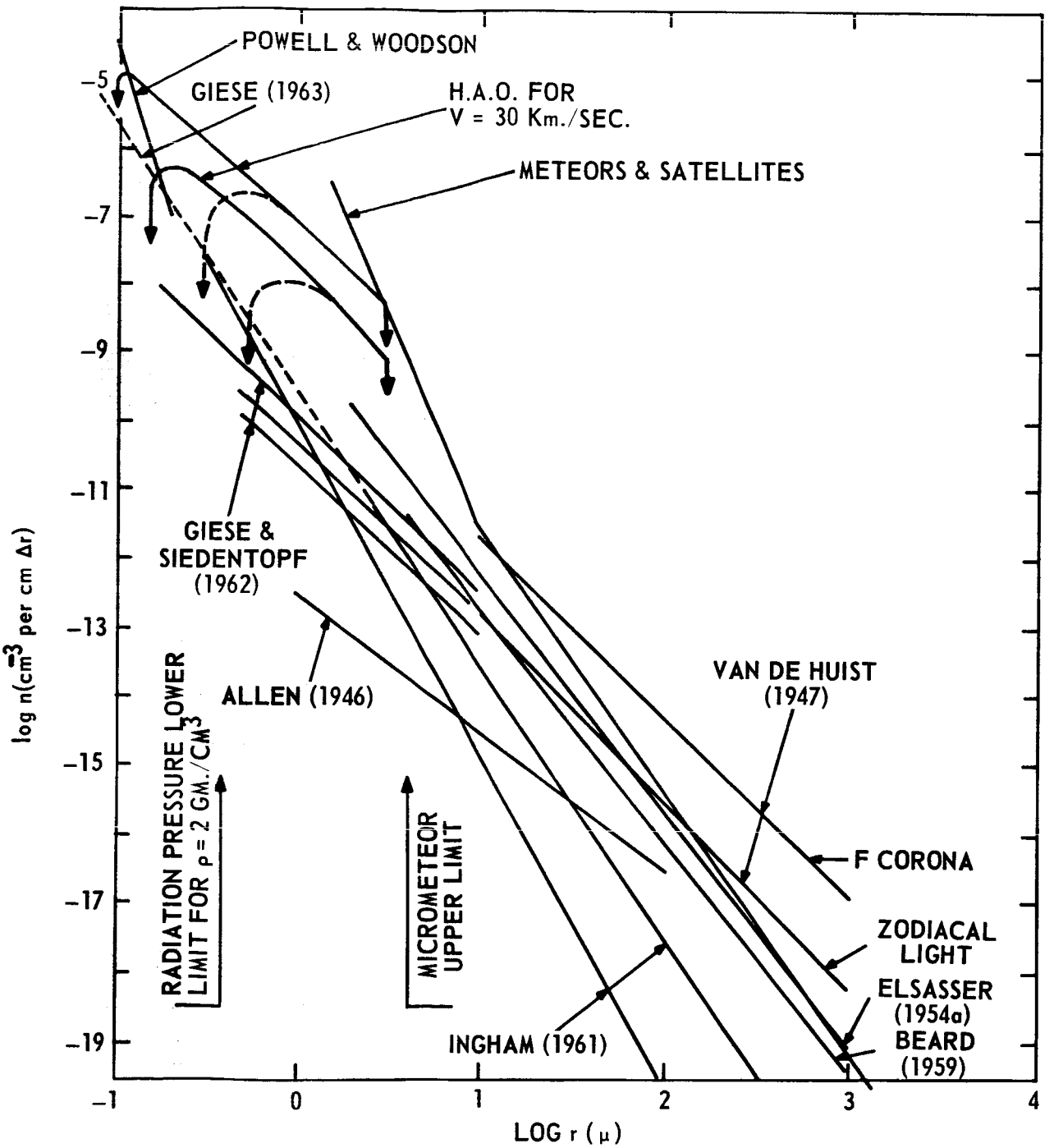


Figure 12. Average Size Distribution Derived from the Belt Model (Powell & Woodson) Compared to Previous Estimates.

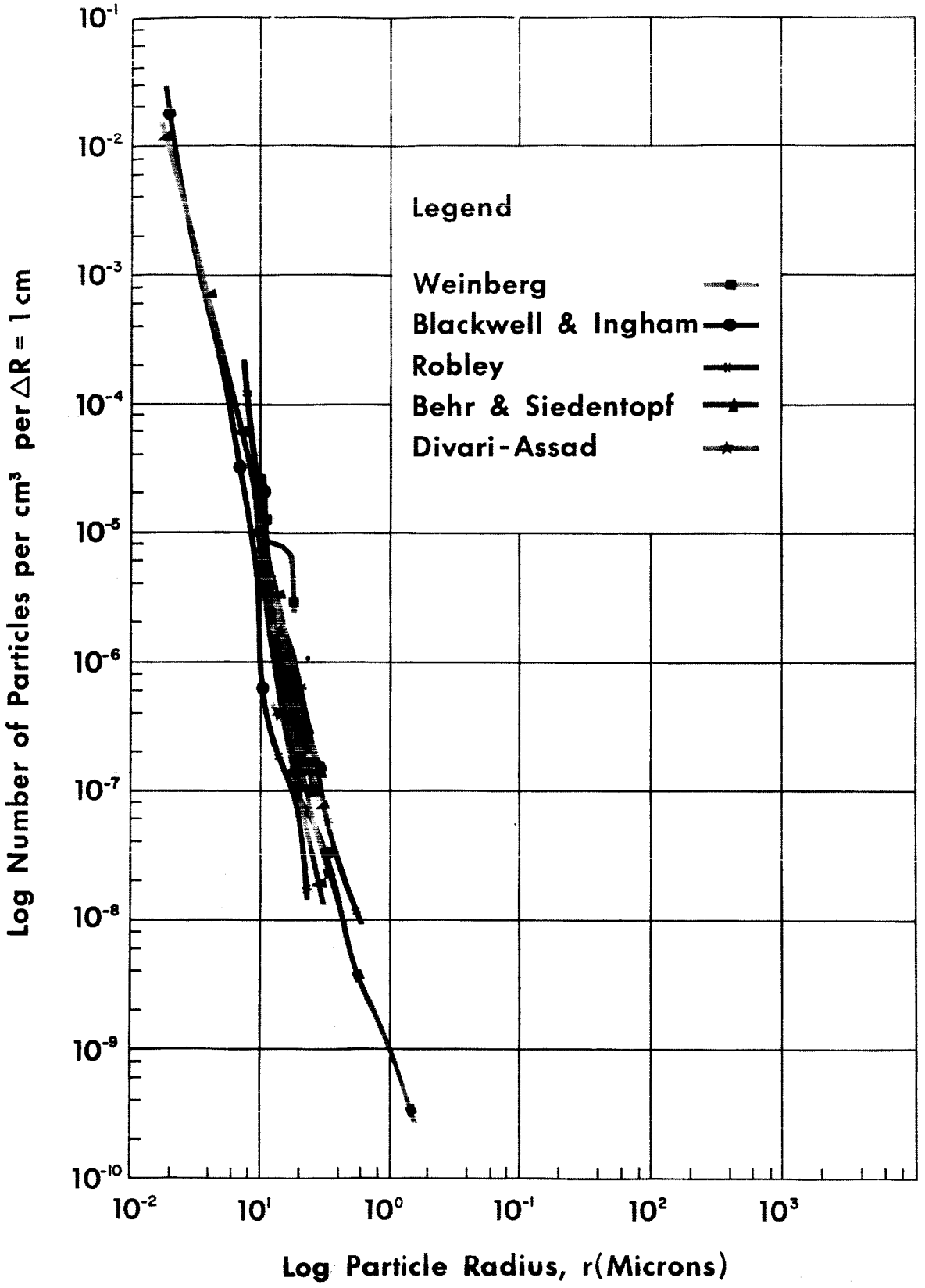


Figure 13. Superposition of All Derived Size Distributions

## 4. THE COLOR OF THE ZODIACAL LIGHT AS ESTIMATED FROM THE BELT MODEL

A unique model of the interplanetary dust ensemble can only be derived from "monochromatic" ($\lambda \leq 50$ Å), three-color observations of the brightness and polarization at all elongations $30^\circ \leq \epsilon \leq 160^\circ$. Such complete observations are not yet available. The validity of our belt model is, therefore, open to question since it was derived from single-color or wideband measurements. However, Tanabe (1967) has measured the absolute brightness of the zodiacal light at elongations $15^\circ \leq \epsilon \leq 40^\circ$ at three wavelengths (4300Å, 5300Å, 6000Å) and Karyagina (1961) has made relative three color measurements at $\epsilon = 40^\circ$-$50^\circ$.

Thus, it is possible to test the validity of the belt model in a preliminary manner by comparing the color of the zodiacal light predicted from the belt model to the measurements of Tanabe and Karyagina at elongations where the single color observations are in coincidence. In this section we give the results of such a comparison using the size distributions derived from the observations of Weinberg.

According to the belt model, the color of the zodiacal light should appear as shown in figure 14. Note that it is bluish at all elongations, slightly bluer than the average measured by Tanabe. However, a comparison with Tanabe's measurements is only valid at $\epsilon = 30^\circ$ where the absolute brightness measured by Tanabe and Weinberg at $\lambda = 5300$Å is the same. At $\epsilon = 30^\circ$ the color as predicted from the belt model can be represented by a color Matrix, $Q(30^\circ)$, the elements of which represent the relative brightness at $\lambda = 4300$Å (top), $\lambda = 5300$Å (middle) and $\lambda = 6000$Å (bottom):

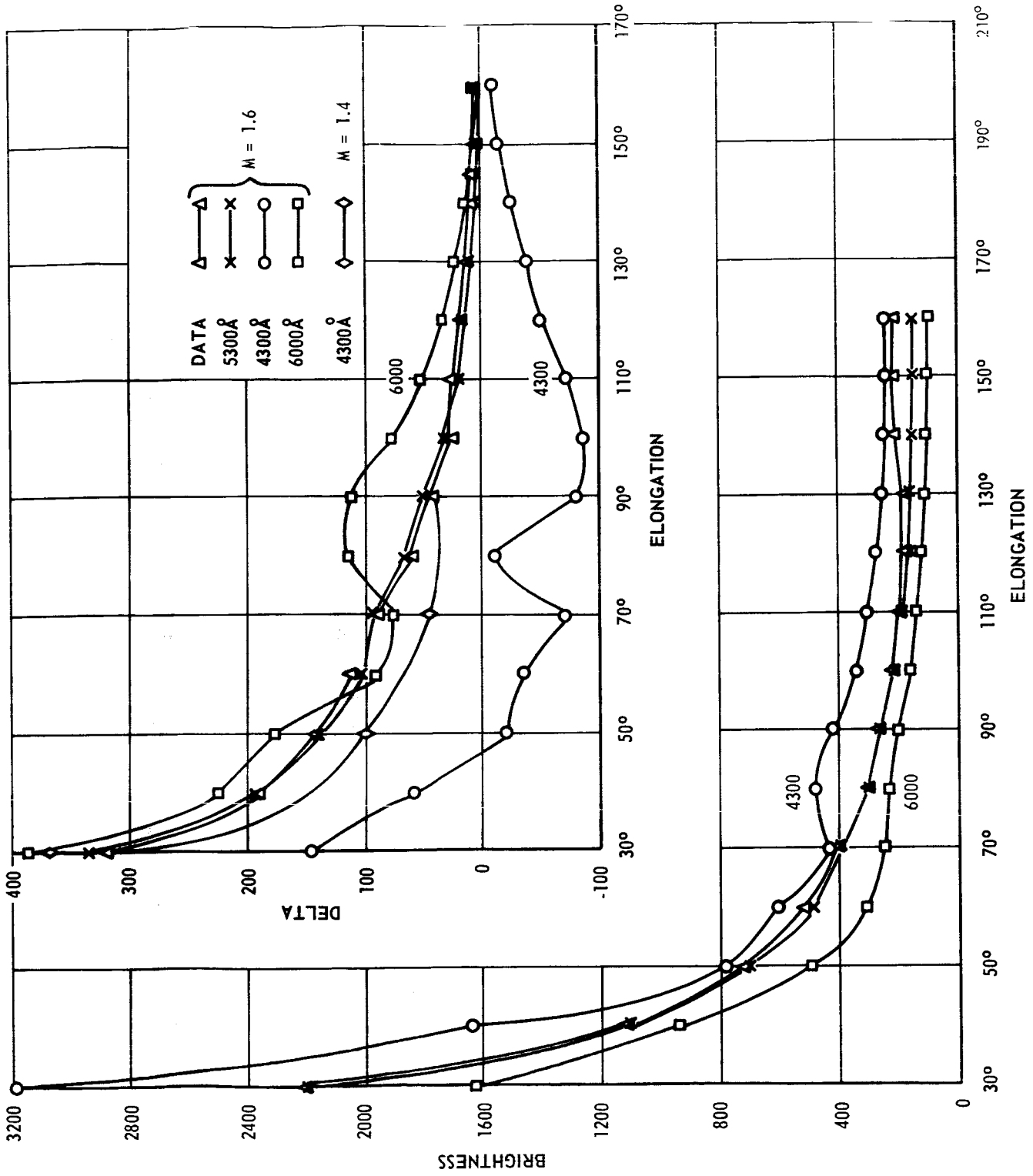


Figure 14. Color of the Zodiacal Light as Predicted from the Belt Model (as derived from Weinberg's single color observations)

$$Q(30^\circ) = \begin{bmatrix} 1.45 \\ 1.00 \\ 0.84 \end{bmatrix} \quad \text{predicted from Weinberg}$$

Tanabe's measurements at $\epsilon = 30^\circ$ can be represented by three such matrices depending upon whether one considers the maximum or minimum

$$\begin{bmatrix} 1.45 \\ 1.00 \\ 0.55 \end{bmatrix} \qquad \begin{bmatrix} 1.15 \\ 1.00 \\ 0.68 \end{bmatrix} \qquad \begin{bmatrix} 0.86 \\ 1.00 \\ 0.91 \end{bmatrix} \qquad \text{Tanabe } \epsilon = 30^\circ$$

Max. Blue  Average  Min. Blue

measured values possible within the constraints of his experimental error.

At $\epsilon \simeq 45^\circ$ the color matrix predicted from the belt model is:

$$Q(45^\circ) = \begin{bmatrix} 1.16 \\ 1.00 \\ 0.75 \end{bmatrix} \quad \text{predicted from Weinberg}$$

Karyagina's measurements over the interval $40^\circ < \epsilon < 50^\circ$ give:

$$\begin{bmatrix} 1.25 \\ 1.00 \\ 0.35 \end{bmatrix} \qquad \begin{bmatrix} 0.91 \\ 1.00 \\ 0.53 \end{bmatrix} \qquad \begin{bmatrix} 0.71 \\ 1.00 \\ 0.75 \end{bmatrix} \qquad \text{Karyagina } \epsilon \simeq 45^\circ$$

Max. Blue  Average  Min. Blue

Thus, the belt model as derived from Weinberg's observations is compatible with the color measurements of both Tanabe and Karyagina and we must tentatively accept the possibility that the zodiacal light is dominated by submicron size particles. The real test will occur when the polarization is measured at three wavelengths over a wide range of elongations. If the dielectric particles have refractive index greater than $m = 1.5$, the polarization at $\lambda = 4300$Å should be negative for $\epsilon > 50^\circ$. If the polarization at $\lambda = 4300$Å turns out to be positive for $\epsilon < 130^\circ$, the average refractive index of the particles must be $m < 1.5$ or the particles must be non-spherical.

## 5. NONSPHERICAL PARTICLES

The foregoing analysis is based on the assumption that the interplanetary dust particles are spherical. But particles formed through natural processes such as collision, grinding, explosion, thermal stress, nucleation-condensation and coagulation are rarely spherical. Consequently, there is some question regarding the accuracy of the deduced size distributions, radial distributions, absolute number density and refractive index of the interplanetary dust as derived from the Belt model. Since the mathematical difficulties involved in solving Maxwell's equations for nonspherical particles are enormous, it is easier to examine the question by comparison with laboratory experiments.

One approach is to measure the scattering from single, nonspherical particles and compare the results with calculations from the Mie theory. Greenberg et al. (1961) and Giese/Siedentopf (1962a) have approached the problem in this manner using microwave analog techniques. Napper and Ottewill (1963) used optical techniques. Unfortunately, an enormous number of measurements for various sizes, refractive indices, shapes, and orientations are required before we can apply single particle experiments to the general problem of analyzing the zodiacal light.

Another approach is to measure the scattering from ensembles containing randomly oriented, polydisperse particles. This approach has been used by Richter (1956, 1962, 1966), Hodkinson (1963) and others (Donn and Powell, 1962; Powell et al.; 1966), by one of two methods.

The first method is to assume that each nonspherical particle in the measured, laboratory size distribution can be characterized by its volume, its longest dimension, or some combination of geometric parameters. The scattering from spheres with similar dimensions is then calculated and compared to the measured scattering. Little et al. (1965) used this method to compare Richter's data with the Mie theory. Napper and Ottewill (1963) used the same technique. The discrepancies in the resulting scattering diagrams for nonspheres and spheres respectively are unpredictable. These discrepancies do not indicate that nonspherical particles scatter differently than spheres. They only indicate that spheres and nonspheres cannot be compared on the basis of a linear relationship between their respective geometric properties.

The single particle measurements show that it is probably impossible to find a single sphere of any size and refractive index which scatters like a single nonsphere of given size and orientation. The resonant peaks in the angular and spectral distribution of the scattered irradiance and polarization, each of which corresponds to the stimulation and interaction of many high order multipoles, is much too sensitive to asymmetries in the boundary conditions (Van de Hulst, 1957).

On the other hand, the scattering from an ensemble containing many nonspheres with different alignments and sizes may average out in such a way that it compares almost exactly with the scattering from some other size distribution of spheres. This has been shown for cubes by Donn and Powell et al. In their experiments, the scattering was measured from various known size distributions of cubes and fourlings. Most of the particles

in these distributions were submicron in size. An equivalent size distribution of spherical particles was then determined by inverting the scattering equations according to the Mie theory. In general, it was rather easy to find an equivalent size distribution of spheres which matched the angular distribution of the scattered irradiance and polarization at one wavelength. The equivalent size distribution of spheres was, in general, different from the measured size distribution of nonspheres. Although these experiments were limited to only a few size distributions and particle shapes, the conclusions are interesting:

a. Large volume shapes such as cubes scatter like spheres (figure 15). The equivalent sphere size distributions derived by inverting the measured angular irradiance and polarization at two wavelengths are nearly identical, thus demonstrating that both the angular and wavelength dependence of large volume particles are similar to spheres. Furthermore, the equivalent sphere size distributions are very close to the actual, measured size distributions of cubes. (On the average, a cube scatters like a sphere with diameter such that the sphere just encloses the cube.)

b. On the other hand, small volume shapes such as needles and fourlings (figure 16) exhibit single color scattering diagrams like spheres, but the equivalent sphere size distribution may differ markedly from the actual size distribution (figures 16 and 17). The fourlings scatter like smaller spheres but there is no linear relationship.

c. Although large volume particles exhibit the same wavelength dependence as spheres, small volume particles do not; i.e., a size distribution of spheres which is equivalent to fourlings at one wavelength is not

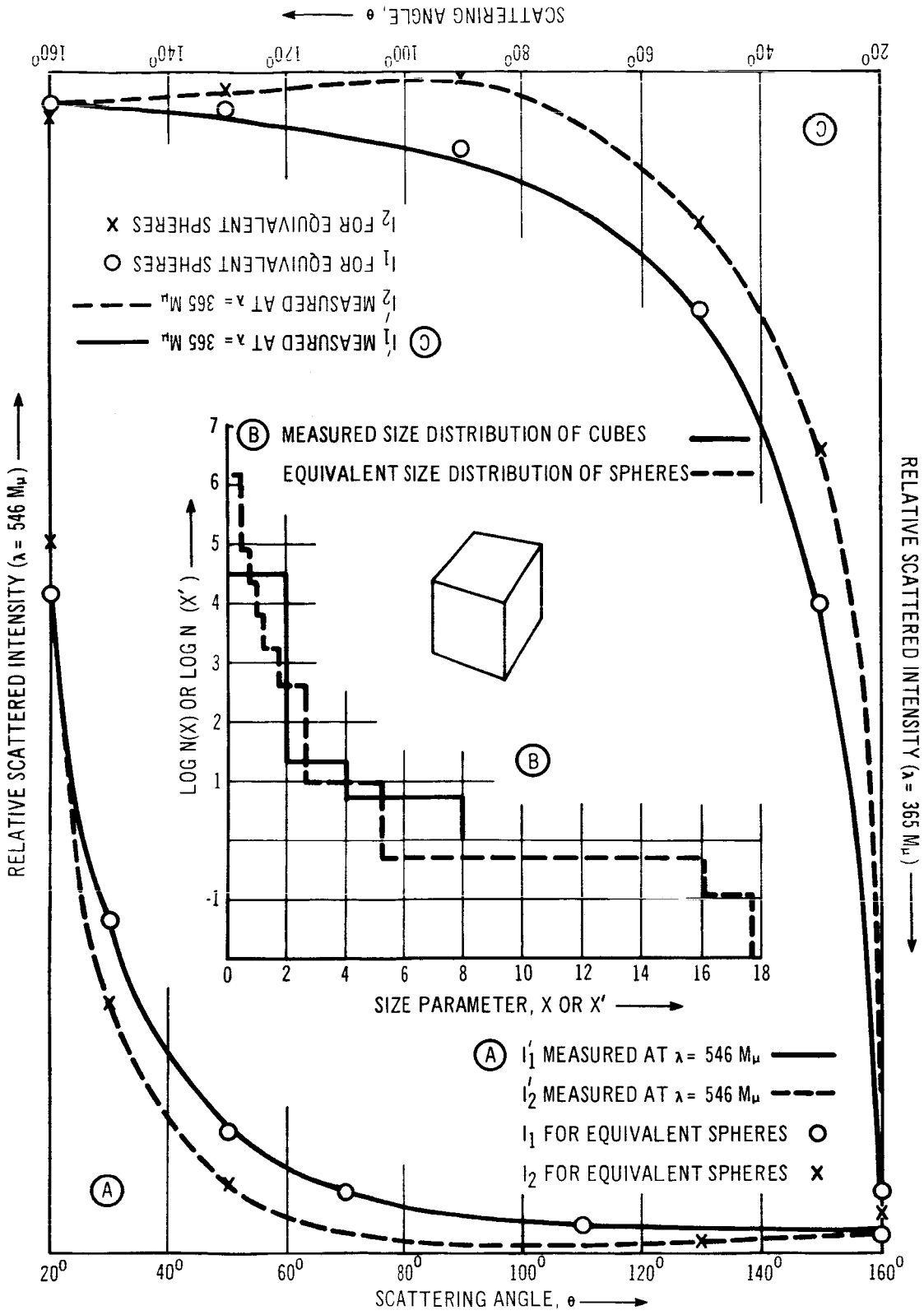


**Figure 15. Optical Character of MgO Cubes**

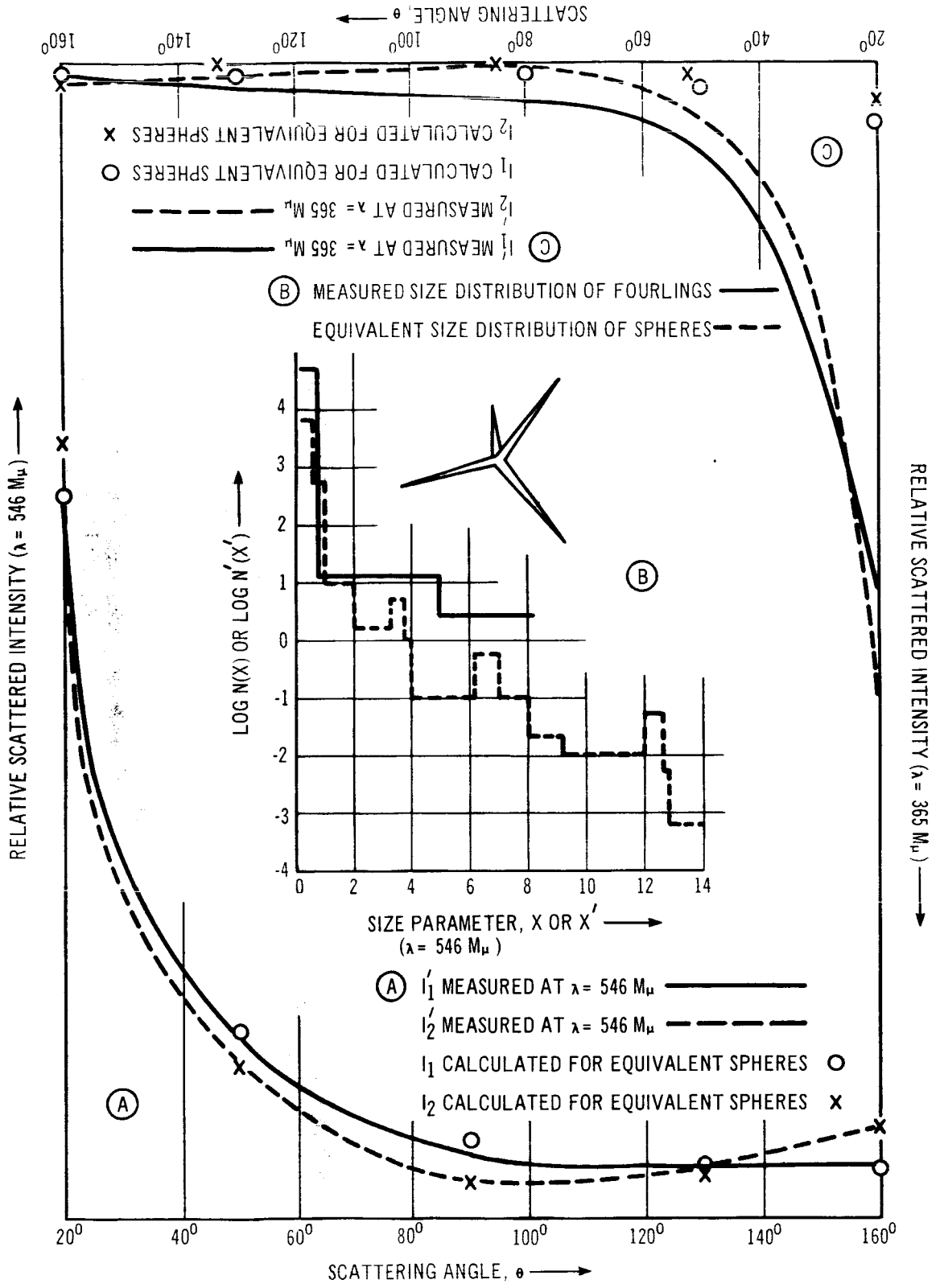


Figure 16. Optical Character of ZnO Fourlings. The equivalent sphere size distribution was constructed to match the angular scattering measured from fourlings at λ = 546 mu. Notice that the scattering from fourlings at λ = 365 mu is not the same as predicted from the equivalent spheres.

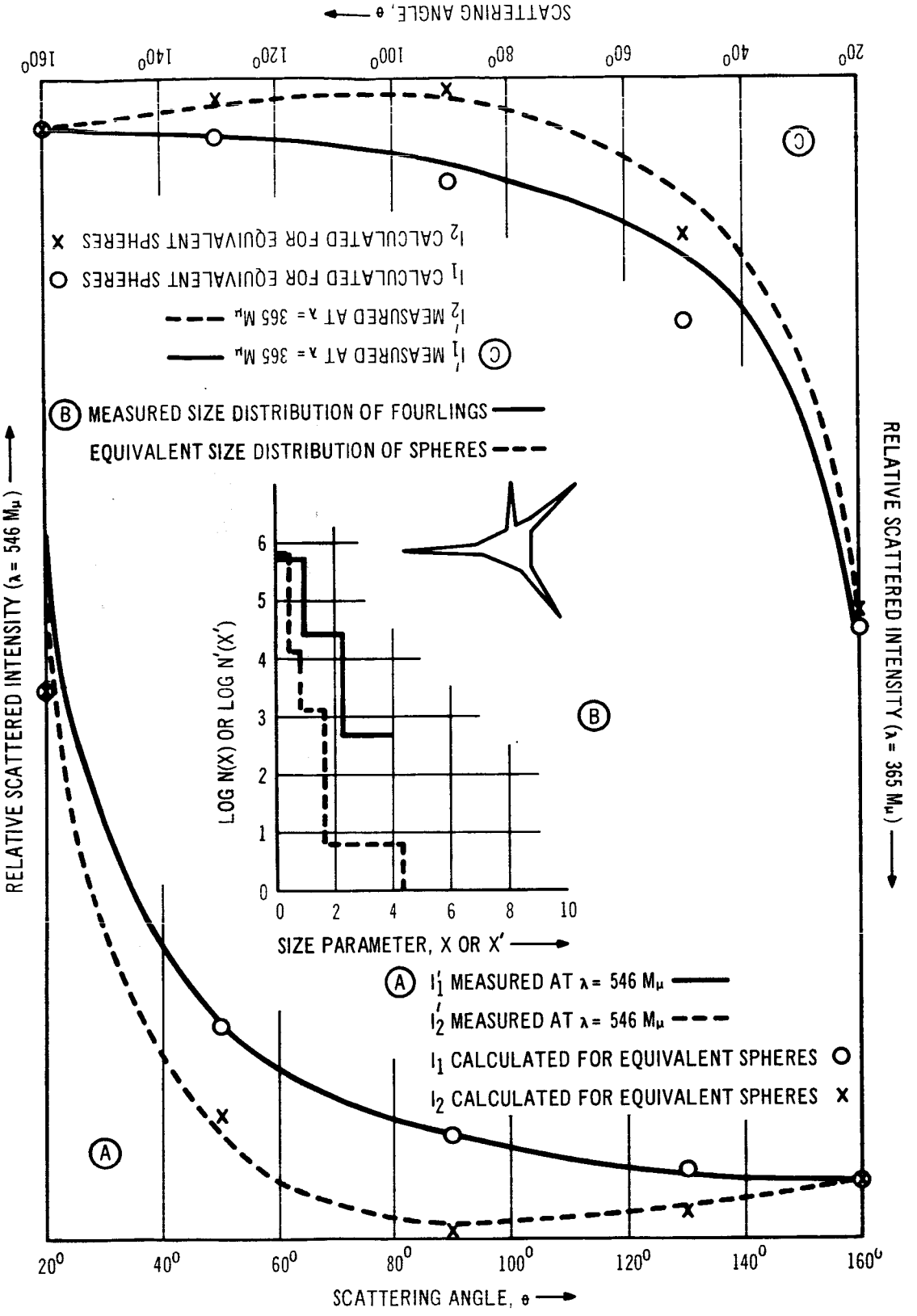


**Figure 17. Optical Character of Imperfect ZnO Fourlings. Although the angular character and wavelength dependence of the light scattered by imperfect fourlings is the same as equivalent spheres (except at 30° < θ < 80° where the wavelength dependence deviates), the equivalent spheres are larger.**

equivalent at another (figures 16 and 17). Thus, small volume particles may look like smaller spheres insofar as single color measurements are concerned, but the wavelength dependence would not be consistent with the Mie theory. In this regard, the optical test for highly nonspherical particles is as follows: first, determine the size distribution of spheres which matches the angular character of the scattered irradiance and polarization as measured at wavelength, $\lambda_1$. Increase the size of all spheres in the equivalent size distribution by $\lambda_1/\lambda_2$. Compare the resulting scattering diagram with angular measurements at $\lambda_2$. If the two compare favorably, the particles are spheres, cubes, octahedra, etc. If there are large discrepancies, especially in the ratio of forward-to-backward scattering, the particles are probably needle-like. We emphasize again that this test only applies to broad size distribution of randomly oriented particles.

The very small size of the particles derived from the Belt model could be due to the fact that the particles are large but needle-like. If so, the usual radiation pressure arguments would be inappropriate because the equivalent ratio of scattering cross-section to mass is unknown for such particle shapes. On the other hand, if the particles are needle-like, the observed color dependence would be incompatible with the Mie theory. Unfortunately, there are not sufficient data concerning the color of the zodiacal light and the wavelength dependence of the polarization to test for needle-like particles. However, the available data are compatible with the idea that most of the particles are large volume types: spheres, cubes,

fat elliposoids and octahedra. Our tentative conclusion is that the particles are not needle-like and, therefore, that the Mie theory is applicable.

## 6. CONCLUSIONS

The general arguments presented are compatible with the following conclusions:

a. All observations indicate that the Zodiacal light phenomenon is due to scattering from submicron particles with radii in the range 0.08 to 1.5 micron.

b. The number density of particles in each size range is approximately constant throughout the ecliptic in the region extending from Venus to Mars.

c. The differences in the observations can be explained by minor changes in the size distribution and composition of the particles in each or all of the belts between Venus and Earth, Earth and Mars, and especially between Mercury and Venus.

d. All observations can be explained by the presence of a dominant fraction of dielectric particles ($1.8 < m < 1.4$) in the regions between Venus and Mars.

e. There is evidence that some iron particles exist in the regions between Mercury and Earth but not beyond Earth. The iron particles tend to be larger (radii between 0.08 and 1.5 microns) than the dielectrics (radii less than 0.3 microns) and the number density of iron particles tends to be less than the number density of dielectrics by a factor of 100.

f. There is evidence that the planets have some effect on the size distribution of the dust near them. Behr and Siedentopf's data cannot be explained without assuming that Venus sweeps out many of the particles near its orbit. More interesting, perhaps, is the fact that an exact fit to

Weinberg's data requires a slightly different size distribution of particles near the Earth's orbit than in the regions of space interior and exterior to Earth.

g. In general concerning the slope: number density vs particle size is steeper than previously expected.

h. The total mass of dust required to explain the zodiacal light observations is in the range $10^{-24}$ to $10^{-26}$ grams per cc.

i. The number density of particles in the region beyond Mars is not sufficient to affect the character of the zodiacal light.

j. Until more accurate three-color observations are made, there is no reason to assume highly nonspherical particle shapes. Spheres, cubes, fat ellipsoids and octahedra all scatter in the same manner. The radiation pressure limit for such shapes should be estimated more accurately (research in progress).

k. The observations analyzed can be explained without any assumptions concerning the number of electrons in the region beyond Mercury. The electron number density as derived from analysis of continuum observations is arbitrary.

l. Further analysis of the presently available zodiacal light observations will not yield unique results. A unique and reliable model of the interplanetary dust ensemble can only be derived from three-color, monochromatic measurements of the brightness and polarization at all elongations; $25^\circ \leq \epsilon \leq 160^\circ$. Measurements in the blue are most important. Monitoring of the three-color brightness and polarization at elongations: $25^\circ \leq \epsilon \leq 40^\circ$ over a period of several months would be valuable. Simultaneous three-color

observations from a satellite and a good earth-bound site such as Haleakala would be very valuable.

m. There is no reason to compare the results from direct impact measurements to deductions from zodiacal light observations in the hope of determining the nature of the near-earth ensemble. The zodiacal light is due to very small particles. Light from particles larger than 1.1μ is swamped by light from smaller particles. Direct impact devices are only sensitive to particles larger than 1 micron (depending on velocity).

n. Geise's analysis (1963) of Blackwell and Ingham's observations using submicron particles is not just an academic exercise as claimed by Elsasser (1965). Only submicron particles fit all the observations in a consistant manner.

o. Obviously, someone should perform a more detailed analysis of effects which counteract radiation pressure.

REFERENCES


ALEXANDER, W.M., C.W. McCracken, J.L. Bohn, (1965), Science, 149, 1240-1241.

ALLEN, C.W. (1947), Mon. Not. Roy. Astron. Soc., 107, 426.

BARBIER, D. (1955) Mem. Soc. Roy. Sci. Liege, 15, 55.

BEARD, D.B. (1959) Astrophysical Journal, 129, 496-507.

BEGGS, D.W., D.E. Blackwell, D.W. Dewhirst, R.D. Wolstencroft, (1964), M.N.R.A.S., 127, 319.

BEHR, A., H. Siedentopf, (1953), Zeits. f. Astrophys, 32, 19-50.

BELTON, M. J. S. (1966) Science, 151, 35-44.

BLACKWELL, D.E., M.F. Ingham, (1961), Mon. Not. Roy. Astron. Soc., 122, 113-127.

BORN, M. and E. Wolf, (1964), Principles of Optics, Pergamon Press, London, 2nd Ed., pp. 633-664.

DIVARI, N.B. and A.S. Asaad, (1960), Soviet Astron. A.J., 3, 832,838.

DIVARI, N.B. (1964) Soviet Ast. J., 7, 547-548.

DIVARI, N.B. and S.N. Kyrlova, (1965), Geomagnetism and Aeronomy, 5, 605.

DONN, B. and R.S. Powell, (1962), "Electromagmetic Scattering", Ed. M. Kerker, Pergamon Press, 151-158.

DONN, B., R.S. Powell, and L. Remy - Battiau, (1967), Nature, 213, 379.

DUFAY, J. (1925) Compt. Rend, 181, 399.

EISASSER, H. (1958), Die Sterne, 9-10, 166-169.
_____(1965), Introduction to Solar Terrestrial Relations, Oriner and Maseland (eds.). Dordrecht, Netherlands, p 149-166.

FESENKOV, V.G. (1963), AIAA J., 1, 1250-1253.

GIESE, R.H. and H. Siedentoph (1962), Informations of the Astronomical Inst. of the U. of Tuebingen, No. 58.

GIESE, R.H. and H. Siedentopf (1962a), Zeitschf. f. Naturforsch, (complete reference unknown).

GIESE, R.H. (1963), Space Science Reviews, 1, 589-611.

GILLETT, F.C. (1966), Report No. 2, Contract NASA (NsG-281-62) and NONR 710(22), U. of Minnesota.

GREENBERG, J.M., N.E. Pederson, and J.C. Pederson (1961), J. Appl. Phys. 32, 233.

HARWIT, M. (1963), J. of Geophys. Res., 68, 2171.

HODKINSON, J.R. (1963), Electromagnetic Scattering, Ed. by M. Kerker, Pergamon Press, 87-100.

HURUHATA, M. (1951), publ. Astron. Soc. Japan, 2, 156-171.

KARYAGINA, Z.V. (1961), Soviet Astronomy-A.J., 4, 828-832.

LILLER, W. (1960), A. J., 132, 867-882.

LITTLE, S.J., B.J. O'Mara, and L.H. Aller (1965) A.J., 70, 346-352.

MIE, G. (1908) Ann. Physik 4, 25, 577.

NAPPER, D.H., R.H. Ottewill (1963), Electromagnetic Scattering, Ed. by M. Kerker, Pergamon Press, 377-386.

PETERSON, A.W. (1961), Astrophys, J., 133, 668-674.

POWELL, R.S., B. Donn, R.R. Circle, D.C. Vogel and P.D. Woodson III (1966), Final Report, NASA Contract NASw-1198.

POWELL, R.S., and B. DONN (1966) to be published, available in limited quantities as Melpar pre-print, Melpar, Inc.

RICHTER, N.B. (1956), Veroff. Sternwarte Sonneberg 2, Heft 6.
_____ (1962), ibid. 5, Heft 4.
_____ (1966), Quart. J. Roy. Astron. Soc. 3, 179.

ROBIEY, R. (1962), Ann. de Geophys., 18, 341-350.

SHAPIRO, I.I., D.A. Lautman and G. Colombo (1966), J. Geophys. Res., 71, 5695-5741.

SMITH, L.L., F.E. Roach, R.W. Owen (1965), Planet Space Sci., 13, 207.

SOBERMAN, R.K. (ed.) GRD Research Notes No. 71., Bedford, Mass.

SOUTHWORTH, R.B. (1964), N. Y. Acad. of Sci. Annals, 119, 54-57.

TANABE, H. (1967), ZLIM Conference, Honolulu, Hawaii

VAN de HULST, H.D. (1947), Astrophys. J., 105, 471.
_____ (1957), Light Scattering by Small Particles, Wiley.

WEINBERG, J.L. (1964a), Summary Report on Zodiacal Light, NASA Publ. HIG-64-11.
_____ (1964b), Annales d'Astrophysique, 27, 713-738.

WOLSTENCROFT, R.D. and L.J. Rose (Jan. 1967), Ap. J.

WYATT, S.P. and F.L. Whipple (1950), Astrophys. J., 111, 134-141

ACKNOWLEDGMENTS

We wish to thank Dr. B. Donn and M. Dubin of NASA for general guidance and criticism. We also wish to thank Drs. J. L. Weinberg and C. W. McCracken whose comments regarding their mistrust of the constant size distribution assumption led to the belt model; and Dr. R. H. Giese whose work gave us the courage to disregard the radiation pressure limit. We also wish to acknowledge the gracious contribution of Mrs. Patricia Lightfoot who programmed the computer. Most of the research was supported by NASA under contracts NASw-1198 and NASw-1206. The remainder was supported by Melpar, Inc.

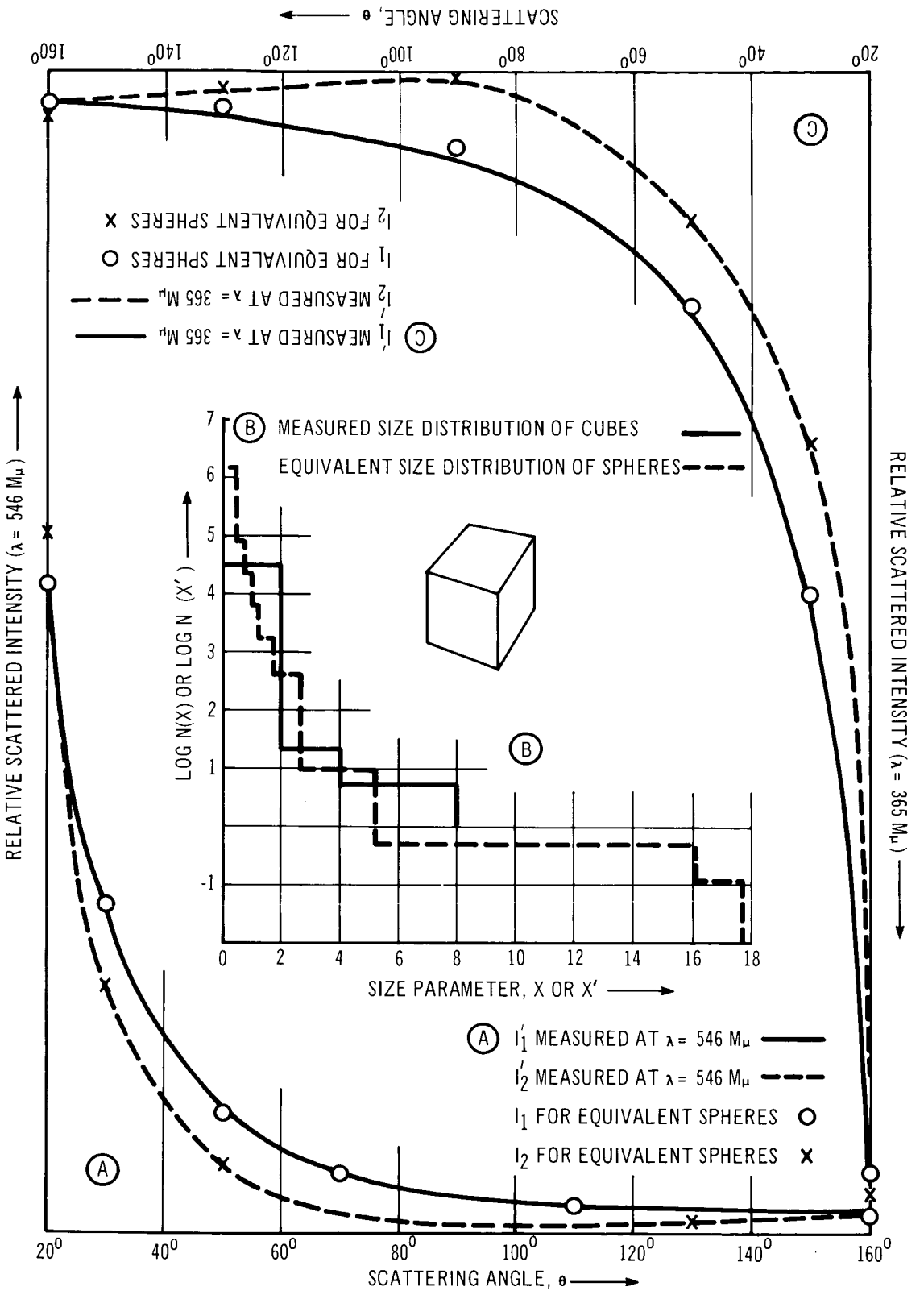
SCATTERING ANGLE, θ
20° 40° 60° 80° 100° 120° 140° 160°
RELATIVE SCATTERED INTENSITY (λ = 365 Mμ)
RELATIVE SCATTERED INTENSITY (λ = 546 Mμ)
(C) I'1 MEASURED AT λ = 365 Mμ
I'2 MEASURED AT λ = 365 Mμ
I1 FOR EQUIVALENT SPHERES
I2 FOR EQUIVALENT SPHERES
(B) MEASURED SIZE DISTRIBUTION OF CUBES
EQUIVALENT SIZE DISTRIBUTION OF SPHERES
LOG N(X) OR LOG N (X')
7 6 5 4 3 2 1 -1
0 2 4 6 8 10 12 14 16 18
SIZE PARAMETER, X OR X'
(A) I'1 MEASURED AT λ = 546 Mμ
I'2 MEASURED AT λ = 546 Mμ
I1 FOR EQUIVALENT SPHERES
I2 FOR EQUIVALENT SPHERES

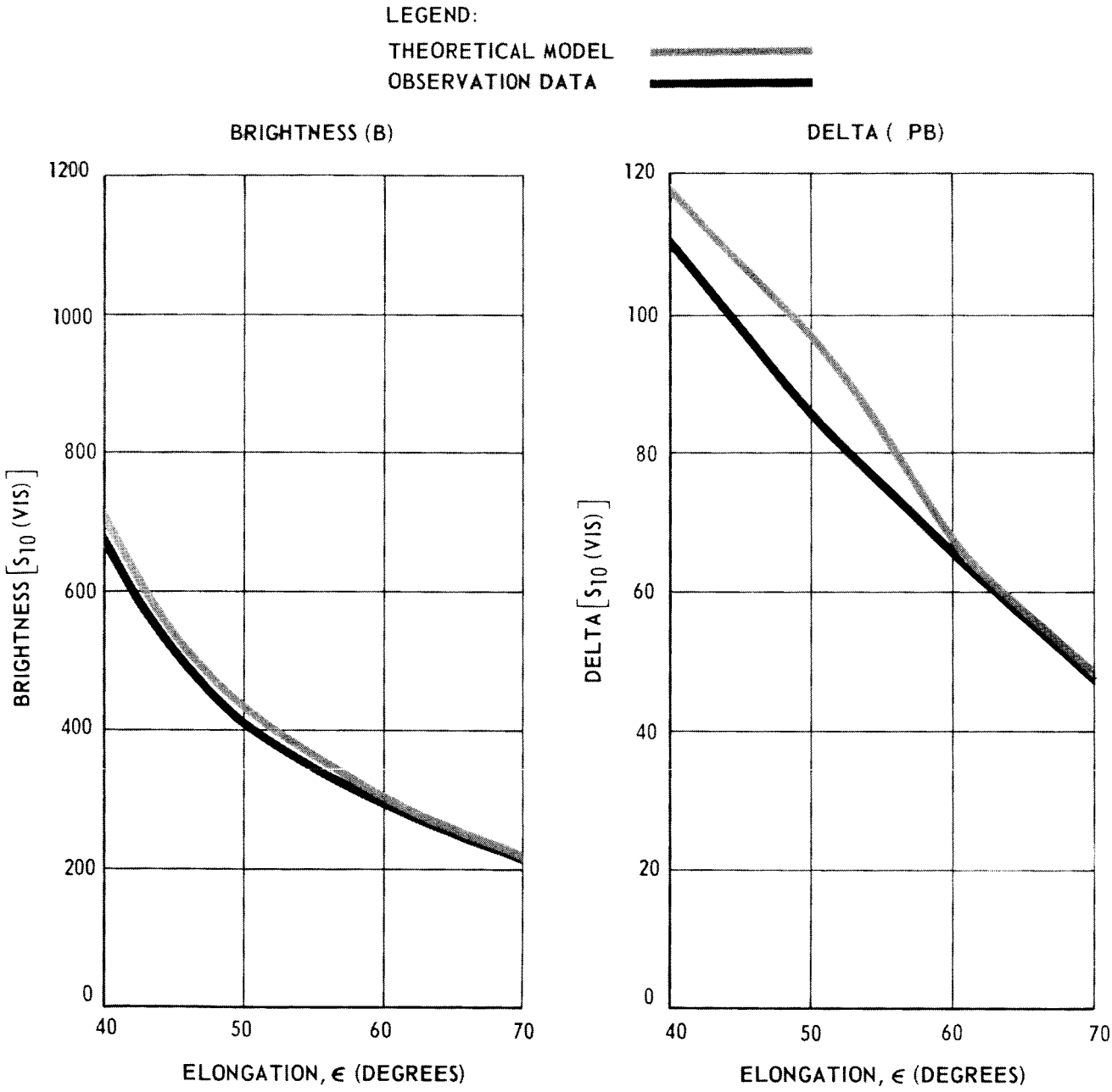
LEGEND:
THEORETICAL MODEL
OBSERVATION DATA
BRIGHTNESS (B)
BRIGHTNESS [S10 (VIS)]
1200
1000
800
600
400
200
0
40
50
60
70
ELONGATION, ϵ (DEGREES)
DELTA ( PB)
DELTA [S10 (VIS)]
120
100
80
60
40
20
0
40
50
60
70
ELONGATION, ϵ (DEGREES)

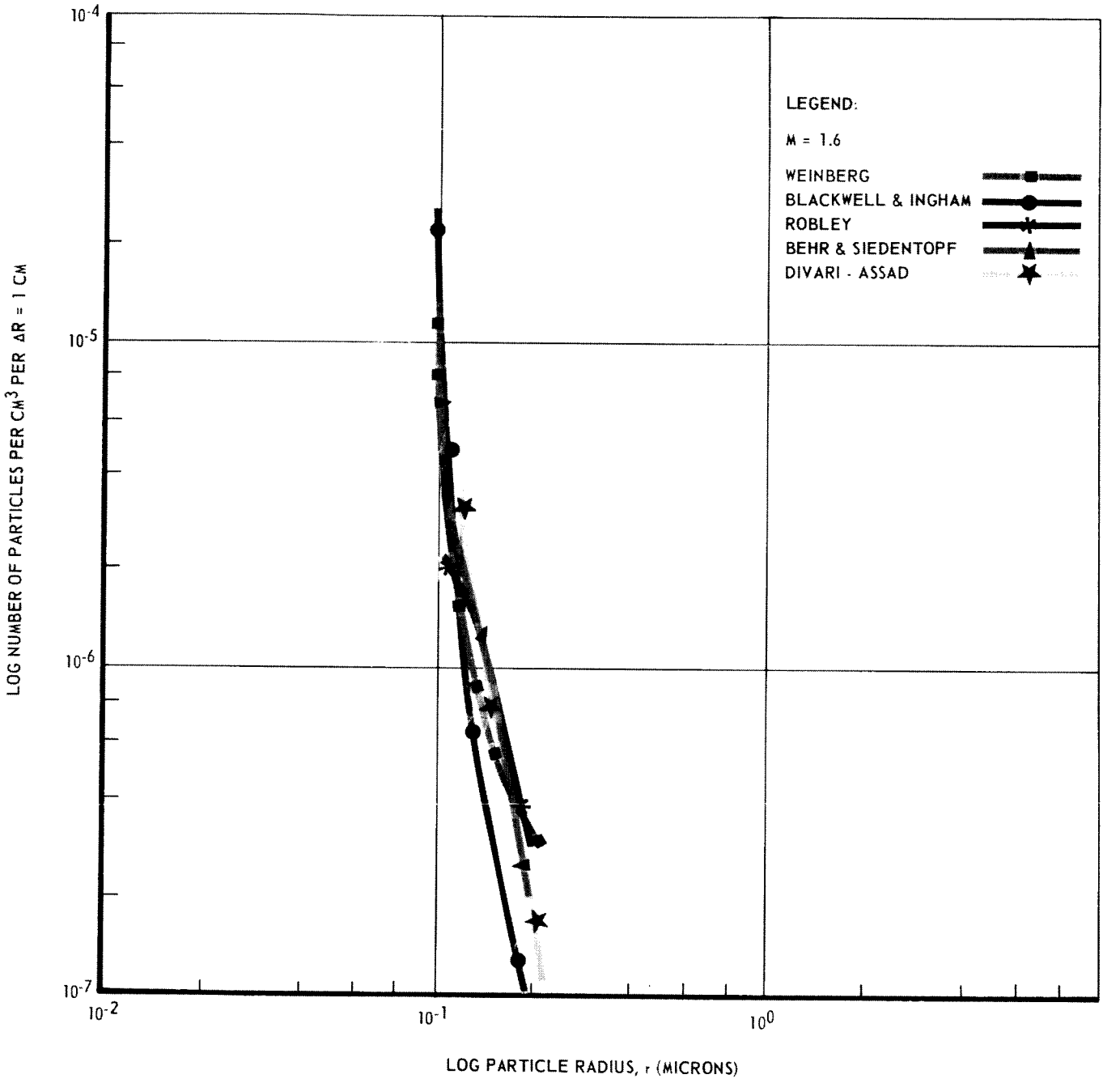
LEGEND:
M = 1.6
WEINBERG
BLACKWELL & INGHAM
ROBLEY
BEHR & SIEDENTOPF
DIVARI - ASSAD
$10^{-4}$
$10^{-5}$
$10^{-6}$
$10^{-7}$
$10^{-2}$
$10^{-1}$
$10^{0}$
LOG NUMBER OF PARTICLES PER $CM^3$ PER $\Delta R$ = 1 CM
LOG PARTICLE RADIUS, r (MICRONS)

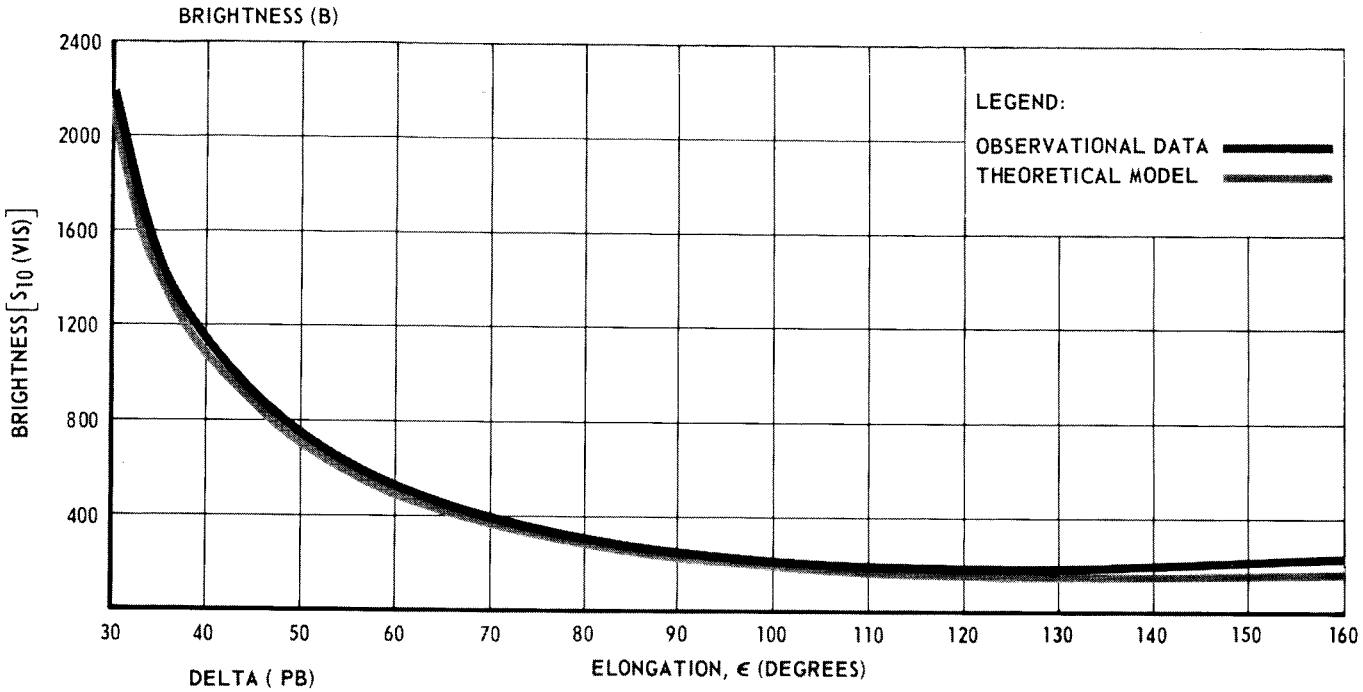
BRIGHTNESS (B)
BRIGHTNESS [S10 (VIS)]
2400
2000
1600
1200
800
400
LEGEND:
OBSERVATIONAL DATA
THEORETICAL MODEL
30
40
50
60
70
80
90
100
110
120
130
140
150
160
ELONGATION, ϵ (DEGREES)

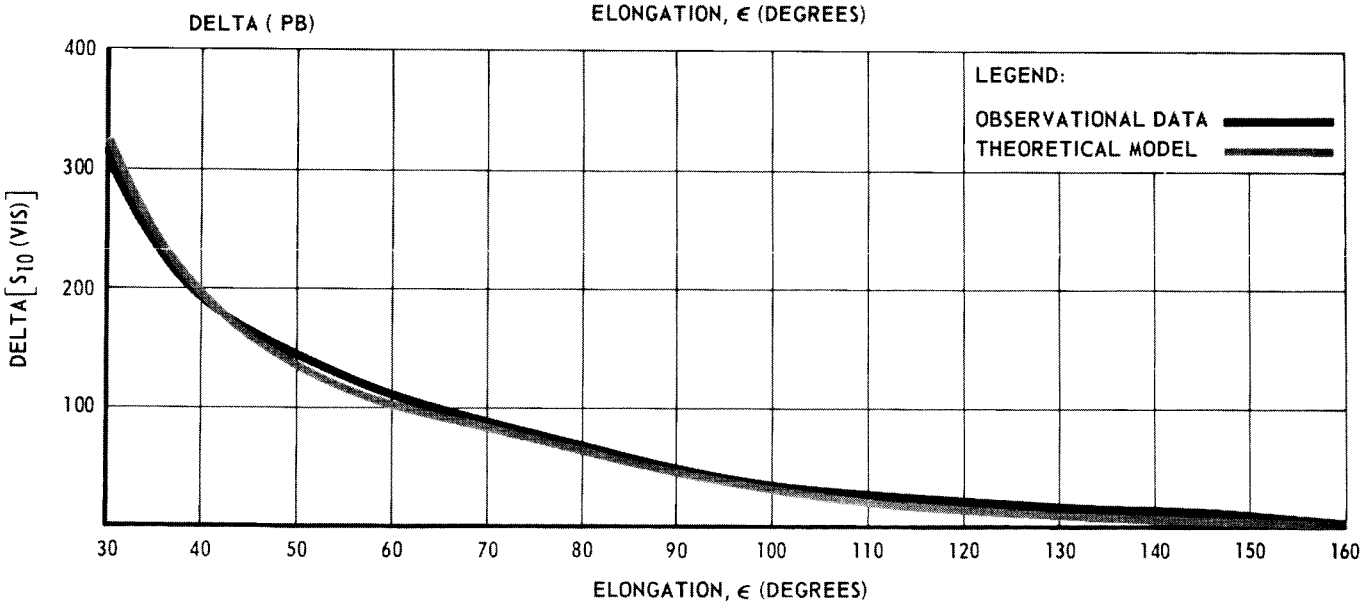
DELTA ( PB)
DELTA [S10 (VIS)]
400
300
200
100
LEGEND:
OBSERVATIONAL DATA
THEORETICAL MODEL
30
40
50
60
70
80
90
100
110
120
130
140
150
160
ELONGATION, ϵ (DEGREES)

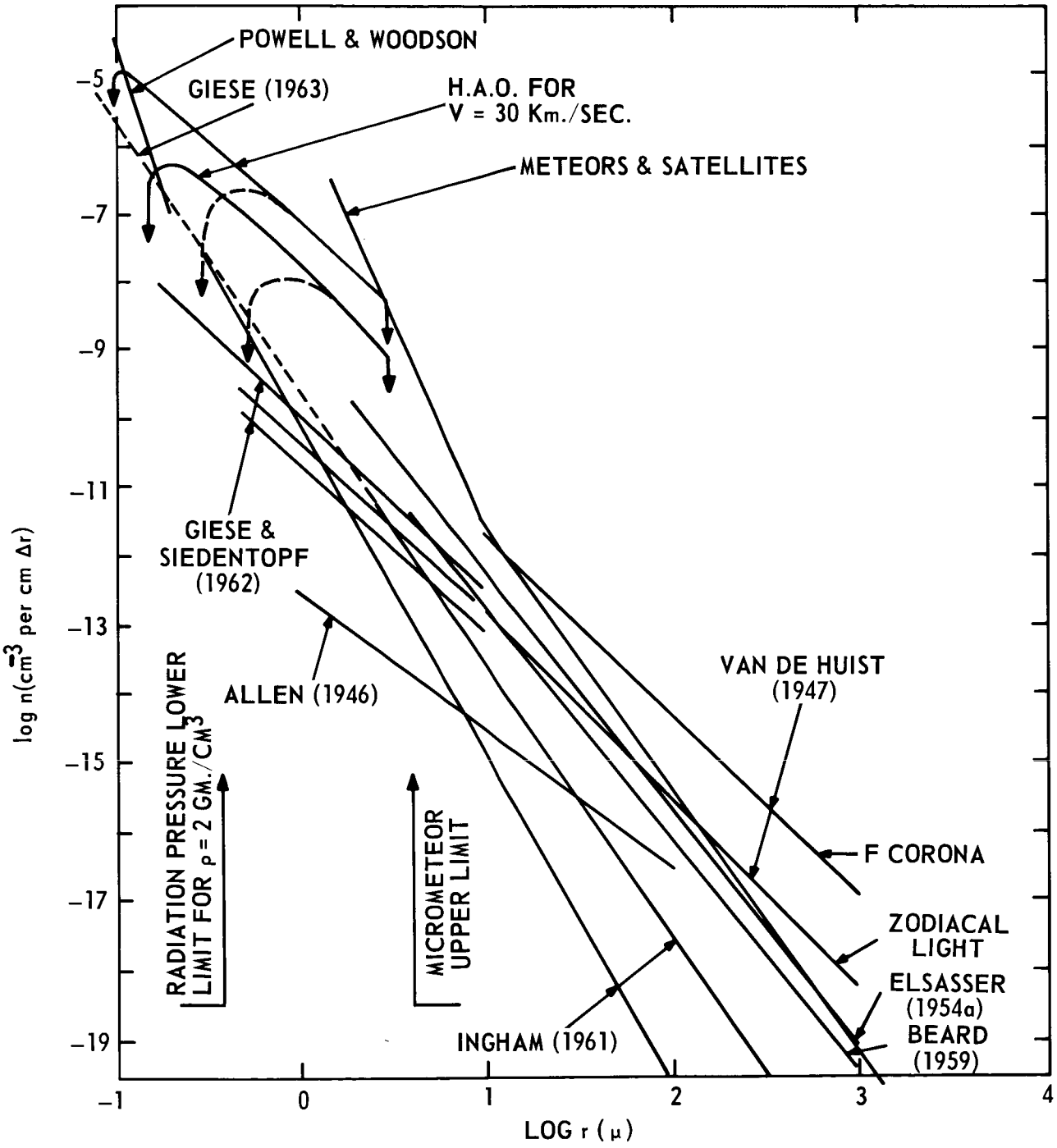
POWELL & WOODSON
GIESE (1963)
H.A.O. FOR
V = 30 Km./SEC.
METEORS & SATELLITES
GIESE &
SIEDENTOPF
(1962)
ALLEN (1946)
VAN DE HUIST
(1947)
F CORONA
ZODIACAL
LIGHT
ELSASSER
(1954a)
BEARD
(1959)
INGHAM (1961)
RADIATION PRESSURE LOWER
LIMIT FOR ρ = 2 GM./CM3
MICROMETEOR
UPPER LIMIT
log n(cm-3 per cm Δr)
LOG r (μ)
-5
-7
-9
-11
-13
-15
-17
-19
-1
0
1
2
3
4

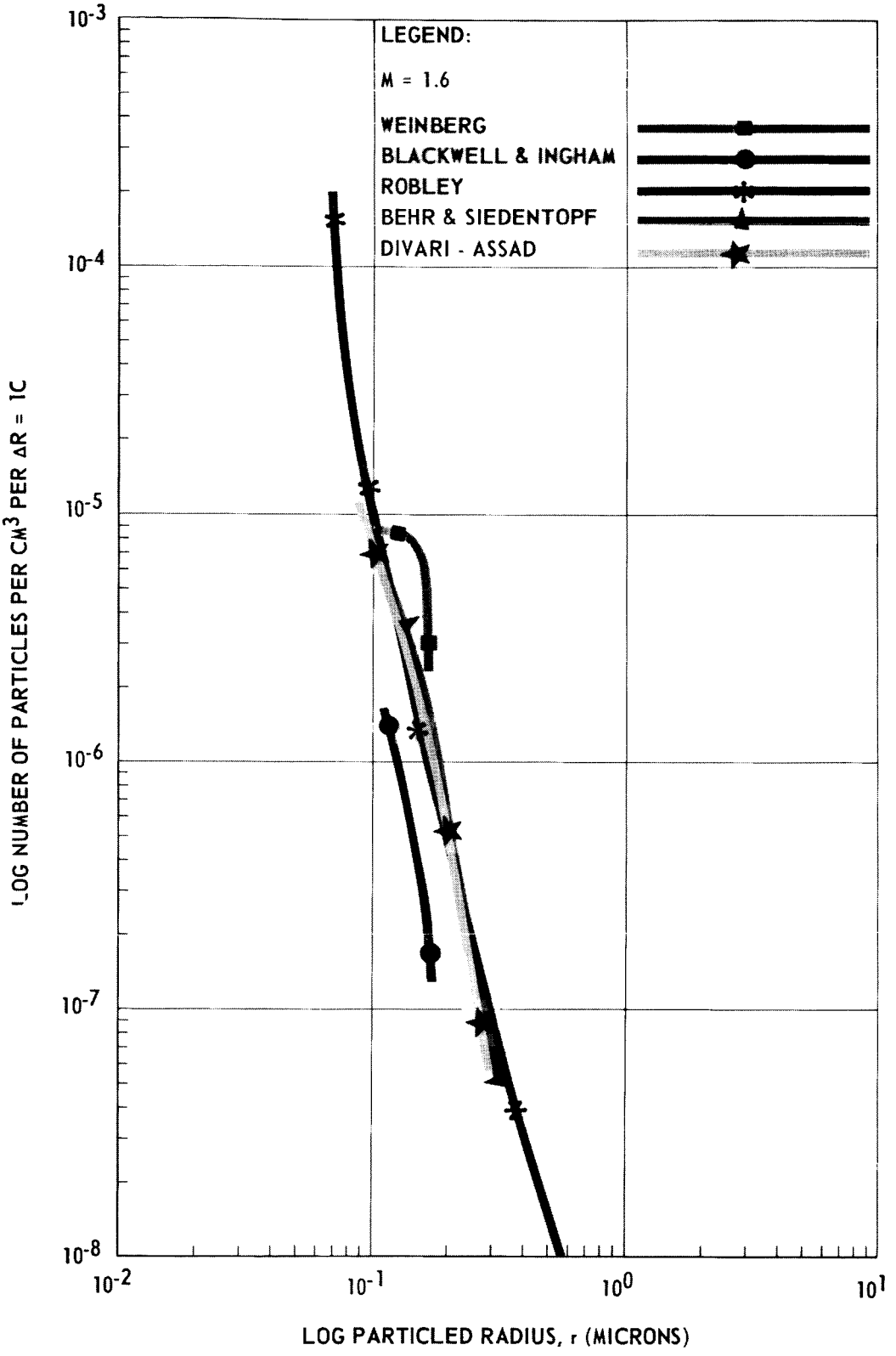
LEGEND:
M = 1.6
WEINBERG
BLACKWELL & INGHAM
ROBLEY
BEHR & SIEDENTOPF
DIVARI - ASSAD
$10^{-3}$
$10^{-4}$
$10^{-5}$
$10^{-6}$
$10^{-7}$
$10^{-8}$
LOG NUMBER OF PARTICLES PER $CM^3$ PER $\Delta R$ = 1C
$10^{-2}$
$10^{-1}$
$10^{0}$
$10^{1}$
LOG PARTICLED RADIUS, r (MICRONS)

# WEINBERG WAVELENGTH SHIFT

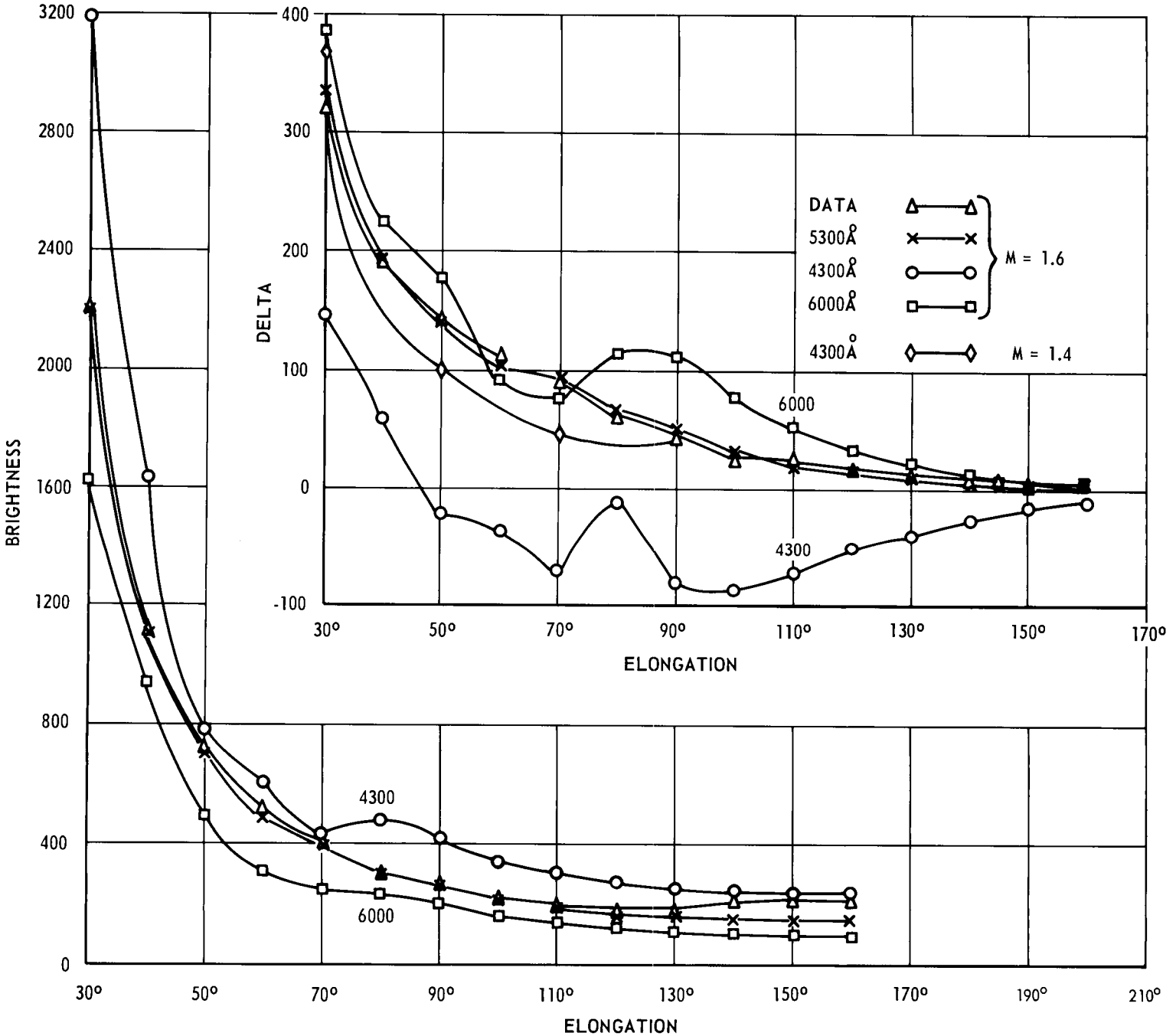

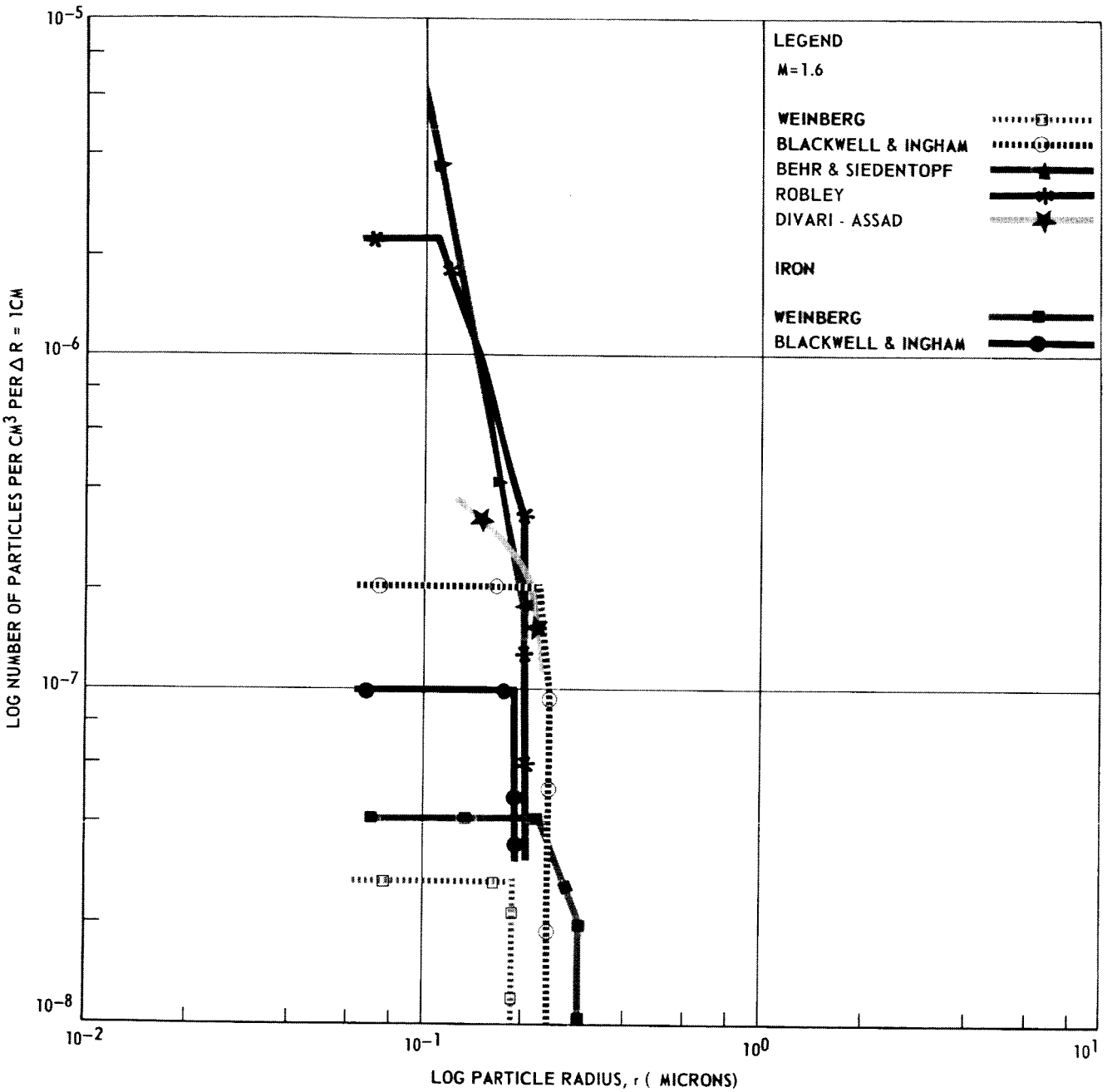
LEGEND
M=1.6
WEINBERG
BLACKWELL & INGHAM
BEHR & SIEDENTOPF
ROBLEY
DIVARI - ASSAD
IRON
WEINBERG
BLACKWELL & INGHAM
LOG NUMBER OF PARTICLES PER CM3 PER Δ R = 1CM
LOG PARTICLE RADIUS, r ( MICRONS)
10−5
10−6
10−7
10−8
10−2
10−1
100
101

RELATIVE SCATTERED INTENSITY (λ = 546 Mμ)
RELATIVE SCATTERED INTENSITY (λ = 365 Mμ)
SCATTERING ANGLE, θ
20° 40° 60° 80° 100° 120° 140° 160°
A
$I_1'$ MEASURED AT λ = 546 Mμ
$I_2'$ MEASURED AT λ = 546 Mμ
$I_1$ CALCULATED FOR EQUIVALENT SPHERES
$I_2$ CALCULATED FOR EQUIVALENT SPHERES
B
MEASURED SIZE DISTRIBUTION OF FOURLINGS
EQUIVALENT SIZE DISTRIBUTION OF SPHERES
LOG N(X) OR LOG N′(X′)
4 3 2 1 0 -1 -2 -3 -4
0 2 4 6 8 10 12 14
SIZE PARAMETER, X OR X′
(λ = 546 Mμ)
C
$I_1'$ MEASURED AT λ = 365 Mμ
$I_2'$ MEASURED AT λ = 365 Mμ
$I_1$ CALCULATED FOR EQUIVALENT SPHERES
$I_2$ CALCULATED FOR EQUIVALENT SPHERES

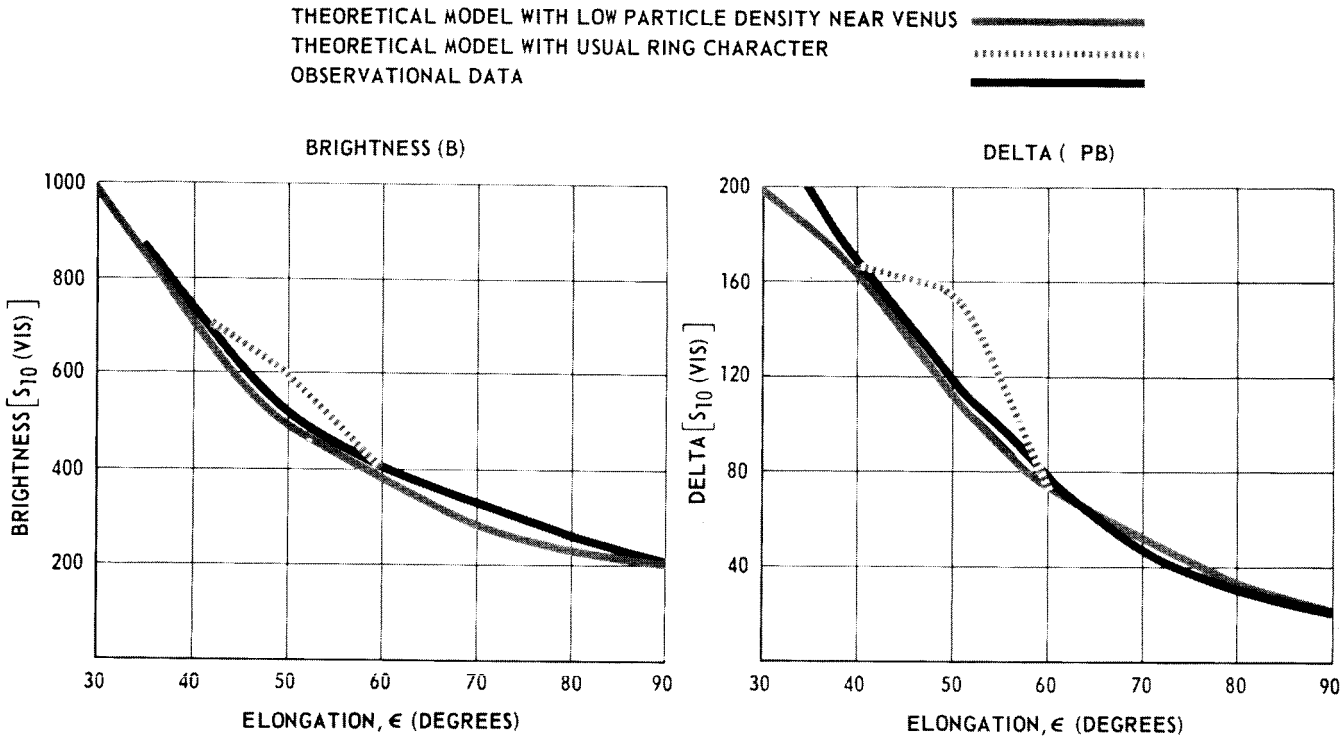
THEORETICAL MODEL WITH LOW PARTICLE DENSITY NEAR VENUS
THEORETICAL MODEL WITH USUAL RING CHARACTER
OBSERVATIONAL DATA
BRIGHTNESS (B)
BRIGHTNESS [S10 (VIS)]
1000
800
600
400
200
30
40
50
60
70
80
90
ELONGATION, ϵ (DEGREES)
DELTA ( PB)
DELTA [S10 (VIS)]
200
160
120
80
40
30
40
50
60
70
80
90
ELONGATION, ϵ (DEGREES)

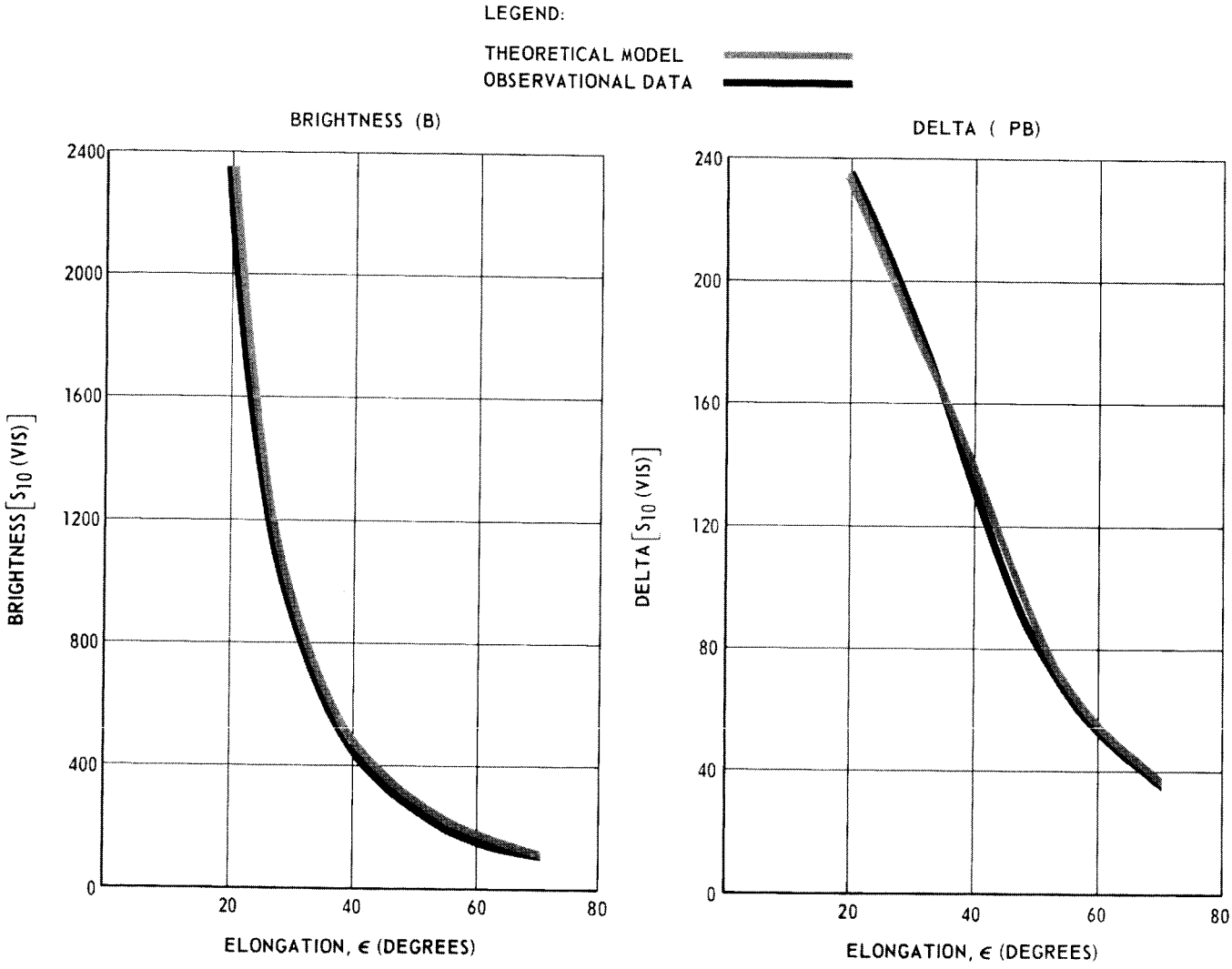
LEGEND:
THEORETICAL MODEL
OBSERVATIONAL DATA
BRIGHTNESS (B)
BRIGHTNESS [S10 (VIS)]
2400
2000
1600
1200
800
400
0
20
40
60
80
ELONGATION, ϵ (DEGREES)
DELTA ( PB)
DELTA [S10 (VIS)]
240
200
160
120
80
40
0
20
40
60
80
ELONGATION, ϵ (DEGREES)

RELATIVE SCATTERED INTENSITY (λ = 546 Mμ)
RELATIVE SCATTERED INTENSITY (λ = 365 Mμ)
SCATTERING ANGLE, θ
20° 40° 60° 80° 100° 120° 140° 160°
A
$I_1'$ MEASURED AT λ = 546 Mμ
$I_2'$ MEASURED AT λ = 546 Mμ
$I_1$ CALCULATED FOR EQUIVALENT SPHERES
$I_2$ CALCULATED FOR EQUIVALENT SPHERES
B
MEASURED SIZE DISTRIBUTION OF FOURLINGS
EQUIVALENT SIZE DISTRIBUTION OF SPHERES
LOG N(X) OR LOG N′(X′)
0 1 2 3 4 5 6
0 2 4 6 8 10
SIZE PARAMETER, X OR X′
C
$I_1'$ MEASURED AT λ = 365 Mμ
$I_2'$ MEASURED AT λ = 365 Mμ
$I_1$ CALCULATED FOR EQUIVALENT SPHERES
$I_2$ CALCULATED FOR EQUIVALENT SPHERES

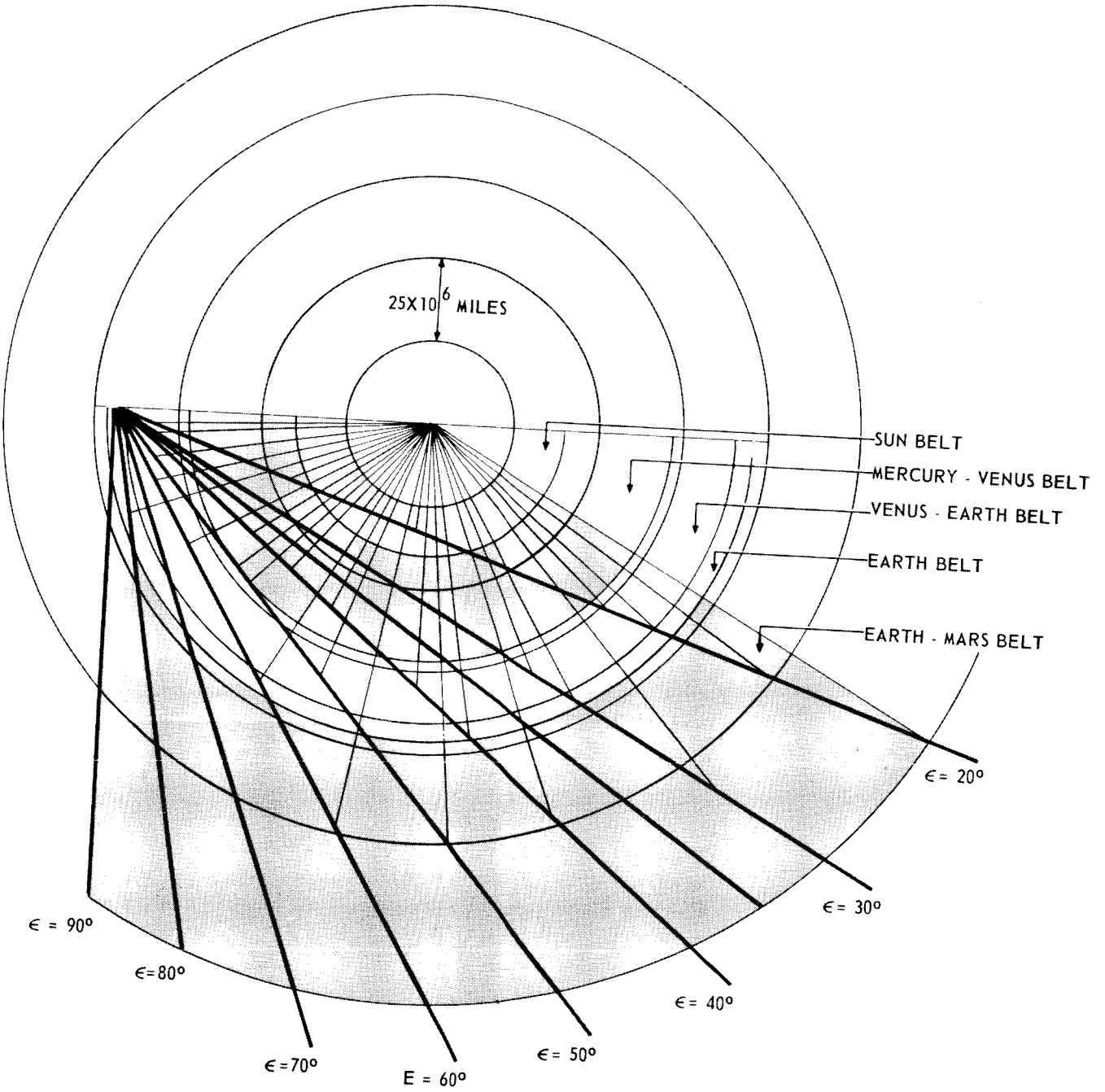
25X10^6 MILES
SUN BELT
MERCURY - VENUS BELT
VENUS - EARTH BELT
EARTH BELT
EARTH - MARS BELT
ϵ = 20°
ϵ = 30°
ϵ = 40°
ϵ = 50°
E = 60°
ϵ = 70°
ϵ = 80°
ϵ = 90°

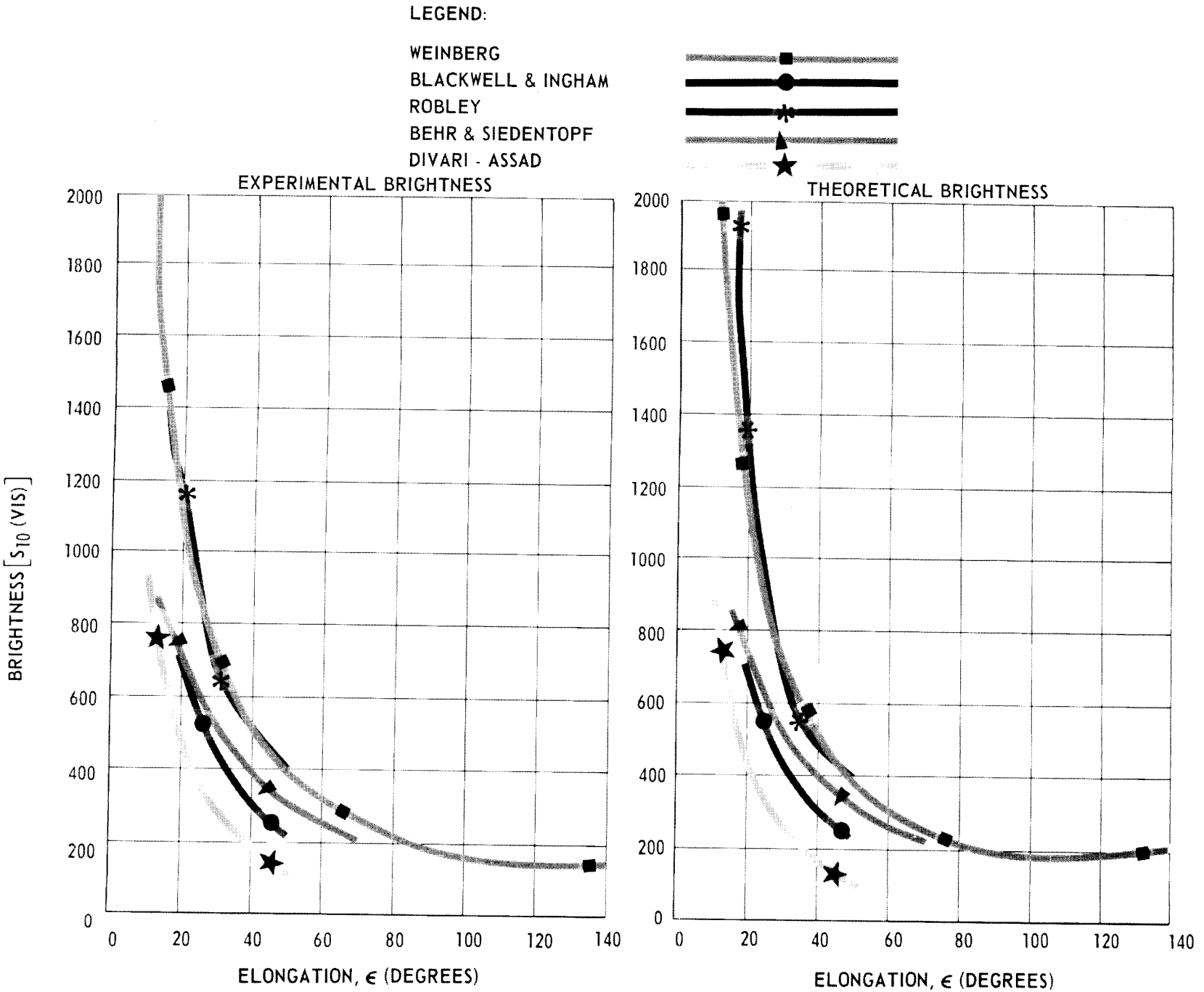
LEGEND:
WEINBERG
BLACKWELL & INGHAM
ROBLEY
BEHR & SIEDENTOPF
DIVARI - ASSAD
EXPERIMENTAL BRIGHTNESS
THEORETICAL BRIGHTNESS
BRIGHTNESS [$S_{10}$ (VIS)]
2000
1800
1600
1400
1200
1000
800
600
400
200
0
0
20
40
60
80
100
120
140
ELONGATION, $\epsilon$ (DEGREES)

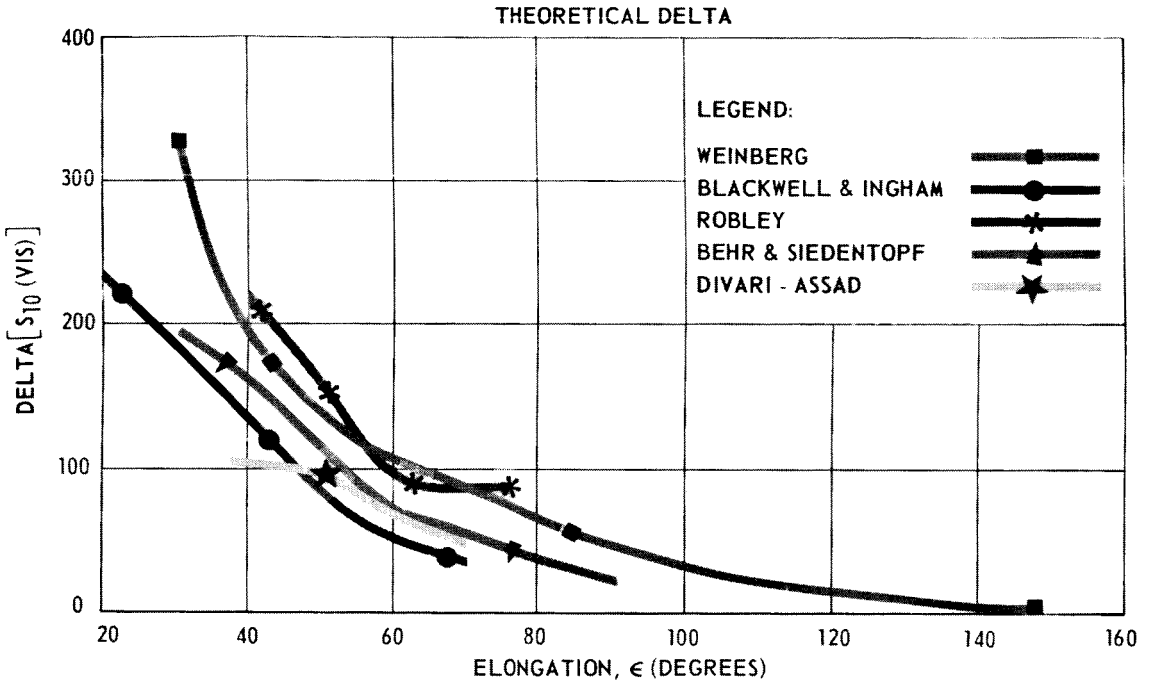
THEORETICAL DELTA
LEGEND:
WEINBERG
BLACKWELL & INGHAM
ROBLEY
BEHR & SIEDENTOPF
DIVARI - ASSAD
DELTA [S10 (VIS)]
400
300
200
100
0
20
40
60
80
100
120
140
160
ELONGATION, ϵ (DEGREES)

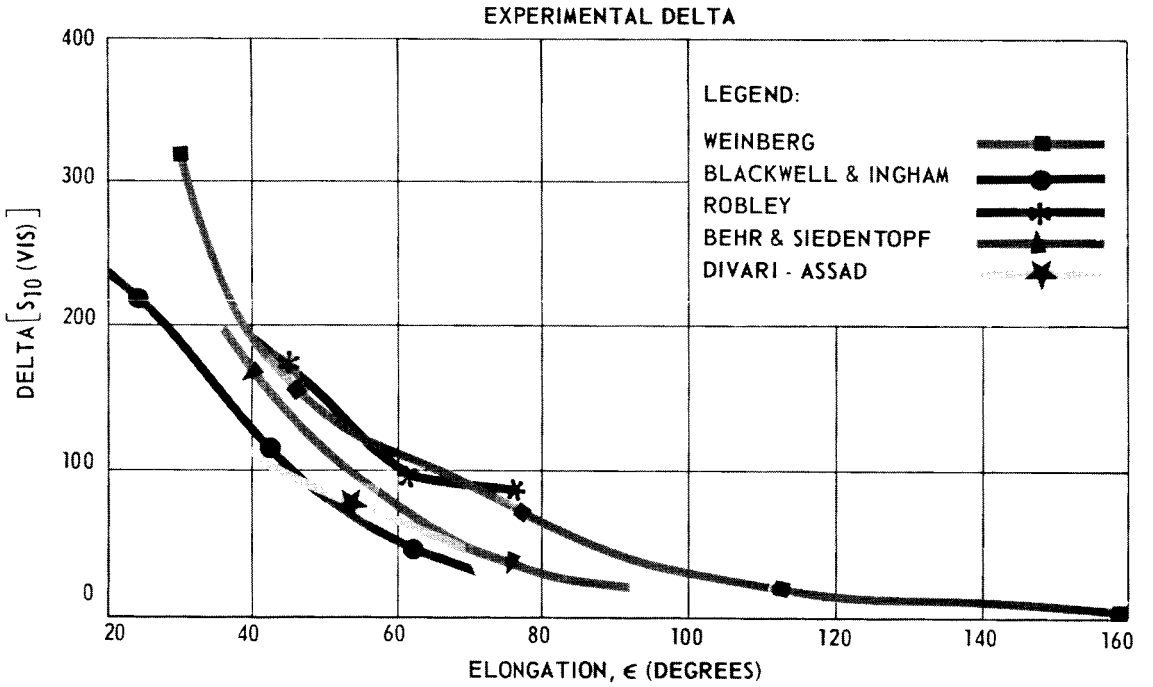
EXPERIMENTAL DELTA
LEGEND:
WEINBERG
BLACKWELL & INGHAM
ROBLEY
BEHR & SIEDENTOPF
DIVARI - ASSAD
DELTA [S10 (VIS)]
400
300
200
100
0
20
40
60
80
100
120
140
160
ELONGATION, ϵ (DEGREES)

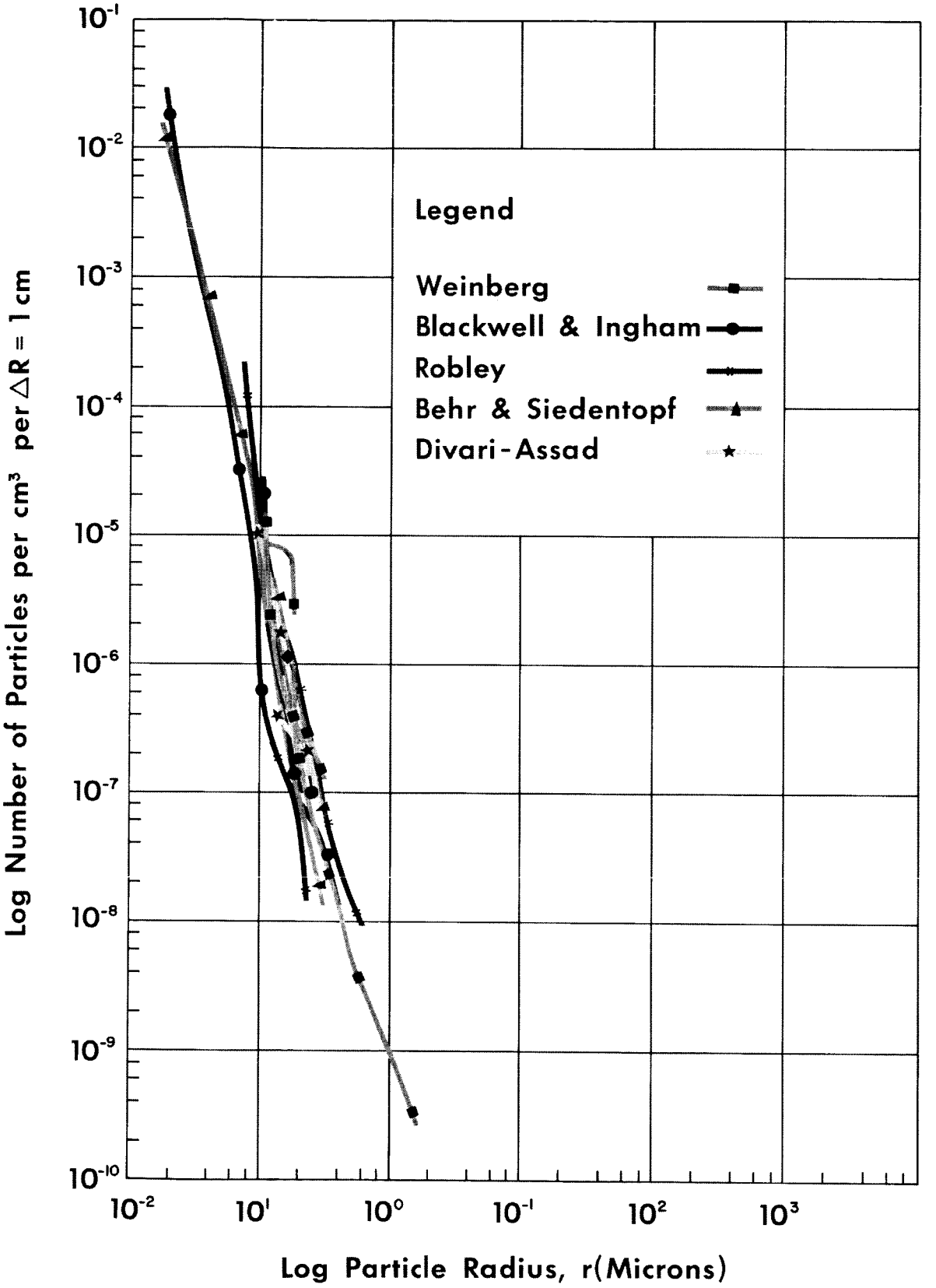
Legend
Weinberg
Blackwell & Ingham
Robley
Behr & Siedentopf
Divari-Assad
Log Number of Particles per cm³ per ΔR = 1 cm
Log Particle Radius, r(Microns)
10⁻¹
10⁻²
10⁻³
10⁻⁴
10⁻⁵
10⁻⁶
10⁻⁷
10⁻⁸
10⁻⁹
10⁻¹⁰
10⁻²
10¹
10⁰
10⁻¹
10²
10³

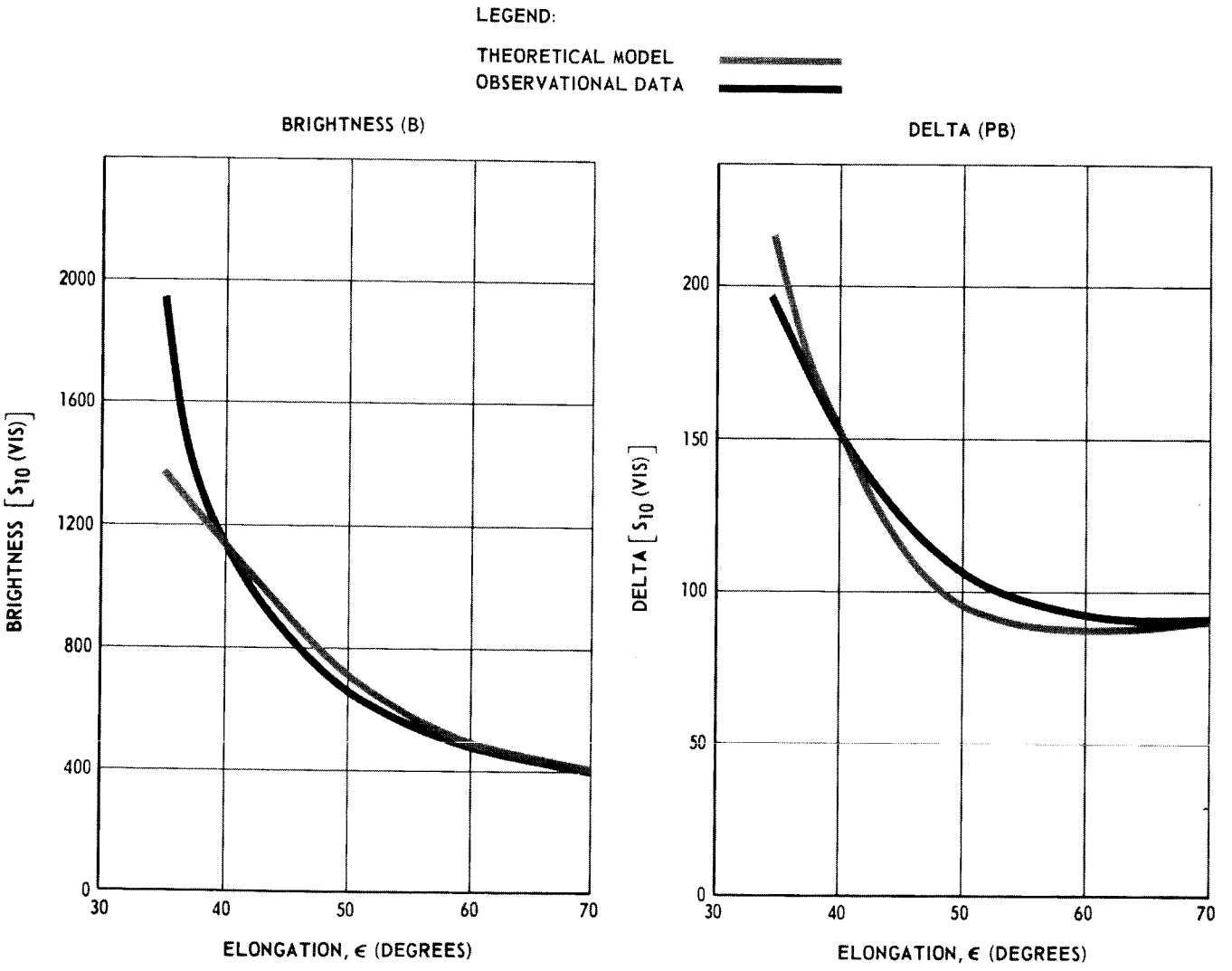
LEGEND:
THEORETICAL MODEL
OBSERVATIONAL DATA
BRIGHTNESS (B)
BRIGHTNESS [$S_{10}$ (VIS)]
2000
1600
1200
800
400
0
30
40
50
60
70
ELONGATION, ϵ (DEGREES)
DELTA (PB)
DELTA [$S_{10}$ (VIS)]
200
150
100
50
0
30
40
50
60
70
ELONGATION, ϵ (DEGREES)

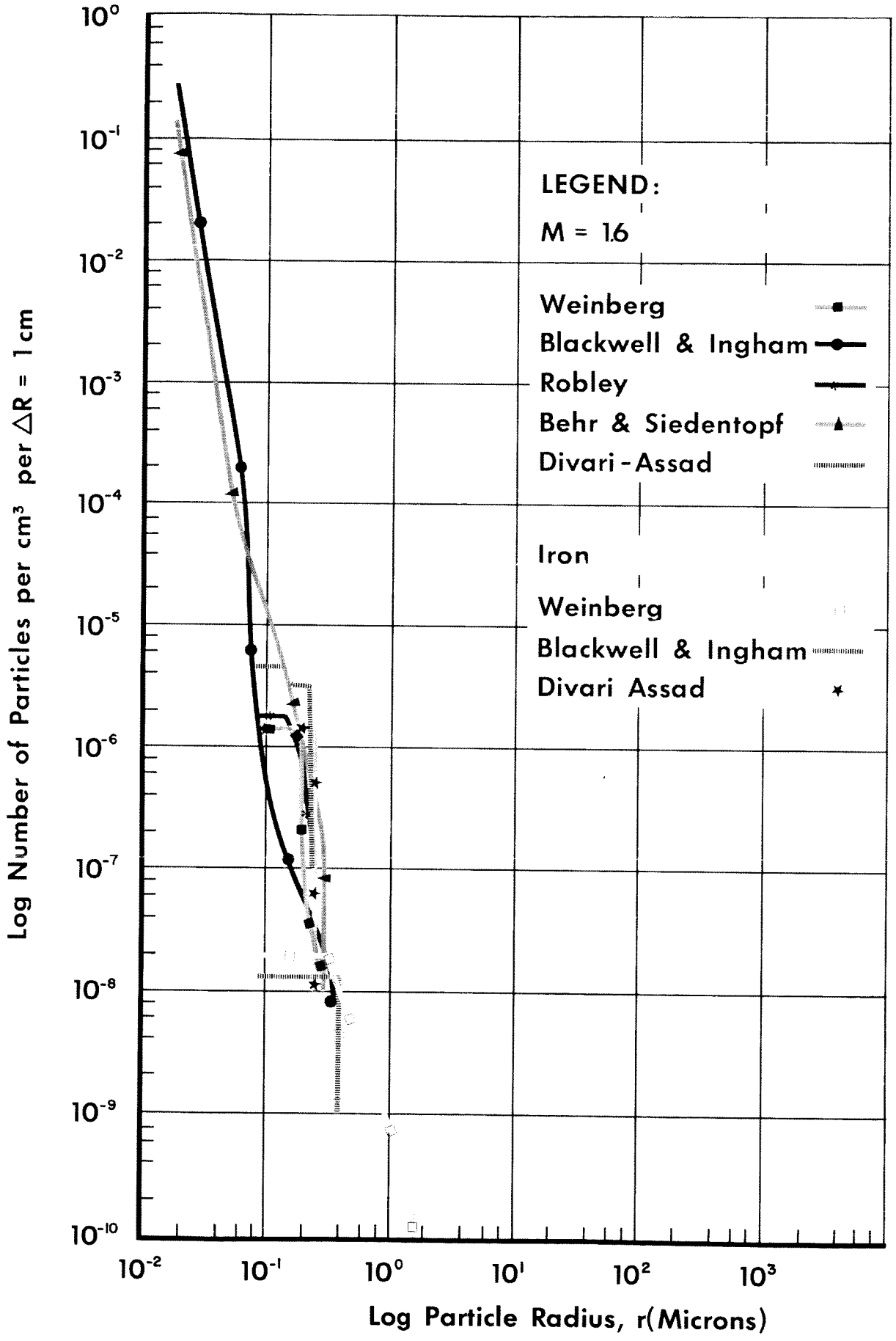
LEGEND:
M = 1.6
Weinberg
Blackwell & Ingham
Robley
Behr & Siedentopf
Divari-Assad
Iron
Weinberg
Blackwell & Ingham
Divari Assad
Log Number of Particles per cm³ per ΔR = 1 cm
Log Particle Radius, r(Microns)
10⁰
10⁻¹
10⁻²
10⁻³
10⁻⁴
10⁻⁵
10⁻⁶
10⁻⁷
10⁻⁸
10⁻⁹
10⁻¹⁰
10⁻²
10⁻¹
10⁰
10¹
10²
10³

# ERRATA

| | |
|---|---|
| All Figures | "ASSAD" should be ASAAD |
| Figure 7 | Word "LEGEND" left out (ref. previous figure) |
| Figure 11 | Word "PARTICLED" should be PARTICLE |
| Figure 12 | 1) Elsasser (1954a). omit 1954a |
| | 2) Ingham (1961). omit (1961) |
| | 3) Allen (1948). omit (1948) |
| | 4) VAN DE HUIST should be VAN DE HULST |
| Page 8 | WEINBERG (1964) should be WEINBERG (1964a) |
| Page 9 | POWELL and DONN (1967) should be POWELL and DONN (1966) |
| Page 11 | WEINBERG (1964) should be WEINBERG (1964b) |
| Page 13 | Title, $\Delta(\varepsilon) = B_1 - B_z$ should be $B_1 - B_2$ |
| Page 15 | 1) WEINBERG (1964) should be WEINBERG (1964b) |
| | 2) "WALSTENCRAFT/ROSE" should be WOLSTENCROFT/ROSE |
| Page 39 | ELLIPOSOIDS should be ELLIPSOIDS |
| Page 40 | $(1.8 < m < 1.4)$ should be $(1.4 < m < 1.8)$ |